Journal of Molecular Liquids 426 (2025) 127465

Contents lists available at ScienceDirect

Journal of Molecular Liquids

journal homepage: www.elsevier.com/locate/molliq

# Sustainable polyphenolate assisted hydrotropic solubilization of riboflavin

Nadja Ulmann *, Johnny Hioe, Didier Touraud, Eva Müller, Dominik Horinek, Werner Kunz *

*Institute of Physical and Theoretical Chemistry, University of Regensburg, Universitätsstrasse 31, 93053 Regensburg, Germany*

ARTICLE INFO

*Keywords:*
Polyphenol
Riboflavin
Stacking
Molecular dynamics
Hydrotrope

ABSTRACT

The solubility of riboflavin is currently thoroughly investigated due to its importance for biological systems. Using real-life experiments and theoretical models, we study the hydrotropic performance and solubilizing mechanism of polyphenolic acid salts and derivatives for the solubilization of riboflavin.

Sodium/choline polyphenolates were both identified as potent hydrotropes for riboflavin via UV–Vis-spectroscopy. Using sodium ferulate and 3,4-dimethoxycinnamate, riboflavin's water solubility can be increased 240 and >2000 times, respectively (molar polyphenolate/riboflavin ratios ≈ 6). Thus, polyphenolates were revealed as more efficient hydrotropes for riboflavin than the usually applied hydrotrope nicotinamide.

Solubilization, surface tension, and dynamic light scattering experiments ruled out the presence of larger well-defined aggregates around riboflavin. The (i) importance of the polyphenolates' π-electron system for riboflavin's solubilization, (ii) reversible bathochromic shifts of riboflavin's absorbance by π-electron-rich solubilizers, (iii) mutual solubilization of riboflavin and of some aromatic sodium carboxylates, (iv) nuclear magnetic resonance (NMR) measurements, and (v) molecular dynamics confirmed π-complexation of riboflavin and aromatic carboxylates as reason for this hydrotropy. Additionally, NMR and NPT simulation indicated sodium polyphenolates to influence the ribityl chain. In water, the overall entropy of riboflavin dissolution is favorable, but in the presence of polyphenolate, the entropy of riboflavin's dissolution is unfavorable and overcompensated by the respective enthalpy.

Finally, both methods hint to a minor influence of the ribityl chain on the dissolution process.

Moreover, real-life experiments and theoretical models state π-electron driven complex formation between the solute riboflavin and the hydrotropic polyphenolates.

## 1. Introduction

### 1.1. What is a hydrotrope?

Regarding the human body with a water content of approximately 65 %, the solubilization of hydrophobic compounds in aqueous medium is obviously a crucial aspect of living [1]. Thus, molecules being able to dissolve hydrophobic compounds in aqueous medium are essential to deliver certain nutrients to our organism.

One important and well-studied class of such solubilizers are surfactants. Based on their amphiphilic nature, surfactants undergo self-aggregation above a critical concentration to form nano-assemblies, in which hydrophobic molecules can be stored or transported. Despite a great solubilizing performance, surfactants are often toxic to aquatic livings, may interfere with membranes and tend to foaming as well as to the formation of liquid crystals [2–4].

To avoid or minimize the latter disadvantages of surfactants, hydrotropes can be utilized. These are small, often slightly amphiphilic molecules, and are now known as solubilizers for sparingly water-soluble compounds, some of them being environmentally benign

*Abbreviations:* $^{13}$C NMR, 13 carbon nuclear magnetic resonance spectroscopy; ca., circa; CAC, critical aggregation concentration; COSMO-RS, conductor-like screening model in real solvents; COSY, correlation spectroscopy; DLS, dynamic light scattering; DMSO-$d_6$, deuterated dimethyl sulfoxide; H, hydrogen atom; $^1$H NMR, proton nuclear magnetic resonance spectroscopy; HMBC, heteronuclear multiple bond correlation; HSQC, heteronuclear single quantum coherence; MD, molecular dynamic; MHC, minimum hydrotrope concentration; NOESY, nuclear Overhouser effect spectroscopy; NaH2PO4, sodium dihydrogen phosphate; NaSCN, sodium thiocyanate; NMR, nuclear magnetic resonance; OH, hydroxyl; OMe, methoxy; PTFE, polytetrafluoroethylene; RF, riboflavin; RF-PO4, riboflavin 5′-monophosphate sodium salt; SDS, sodium dodecyl sulfate; SXS, sodium xylene sulfonate; wt.%, weight percent.

* Corresponding authors.
*E-mail addresses:* Nadja.Ulmann@ur.de (N. Ulmann), Werner.Kunz@ur.de (W. Kunz).

https://doi.org/10.1016/j.molliq.2025.127465
Received 25 October 2024; Received in revised form 6 March 2025; Accepted 25 March 2025
Available online 28 March 2025

[5,6]. Hydrotropes, such as sodium xylene sulfonate, nicotinamide, urea, γ-valerolactone, citrate, and caffeine are currently intensively investigated as green solubilizers [7]. Being mostly of natural origin and considerably less amphiphilic than surfactants, hydrotropes are claimed to be less toxic and irritant [8–10]. The more weakly pronounced amphiphilicity of hydrotropes leads also to a weaker surface-activity when compared to surfactants. Further, hydrotropes do not form liquid crystals and foam considerably less than surfactants [2,11]. Nevertheless, as elucidated by Mehringer et al., via elongation of the hydrophobic part of hydrotropic salts, the transition from hydrotropes to surfactants is fluid [12]. Still, a hydrotrope's solubilization mode cannot be generalized as in the case of surfactants. This originates from the manifold nature of hydrotropes. Usual ones are slightly amphiphilic and thus tend to aggregate above a critical aggregation concentration, mainly in the presence of hydrophobic solutes, while others are only slightly amphiphilic and are characterized by polar groups or aromatic moieties [13,14].

Currently, three mechanisms are suggested for hydrotropic solubilization processes. These are complexation of the solute by the hydrotrope, salting-in due to their ability to alter the water-structure and aggregation/pre-cluster formation [13,14]. In a particular case, the nature of the hydrotrope and the structure of the solute define the actual solubilizing mode. Therefore, hydrotropes are claimed to be highly selective solubilizers, which can be advantageous for extraction processes or certain separation processes [7].

One reason for the diverse action of hydrotropes is that not all water-insoluble compounds are solely unpolar. Thus, cellulose, indigo or vitamin K3 are poorly or even not water-soluble despite bearing polar functional groups [15–17]. Hence, contrary to surfactants, hydrotropes do not only solubilize mainly unpolar organic solutes, but can also act as solubilizers for compounds with intermediate character.

As small, powerful, often natural and lowly or non-toxic versatile molecules, hydrotropes are a tool of green chemistry and compete with green solvents as well as natural deep eutectic and allow for aqueous solutions. Some hydrotropes can easily compete with the mentioned alternatives, in terms of low toxicity, economic concerns, non-flammability, and eco-friendliness [18].

### 1.2. Riboflavin – Vitamin B2

Riboflavin (RF), see Fig. 1, is a vitamin, which is involved in many biological redox-reactions [7–9]. The vitamin is widely used in pharmacy, such as for migraine, cancer and Parkinson treatment [19–22]. Due to its at least sparing water solubility ($0.27 \pm 0.02$ mmol·kg$^{-1}$), RF is excreted via the urine and toxification with this vitamin is improbable [23–25]. Hence, RF is a common nutritional supplement and yellow coloring agent for ice cream, confectionery, meat, dairy products, and beverages and the demand on RF has risen over the years [26,27]. RF's low solubility in various solvents can be obstructive for the yield in its biochemical synthesis, which depends on the reactants' and products' solubility. Moreover, RF's solubility limitations are disadvantageous for its injection or usage as dietary supplement [22,28,29]. Additionally, RF takes a long time to be dissolved in water.

RF is an interesting solute as it has a rather polar molecular structure but has only poor water solubility. Hence, RF's polarity does not rule its solubilization on the one hand but impedes its solubilization by surfactants on the other hand.

Coffman and Kildsig considered nicotinamide and urea as potent hydrotropic solubilizers for RF. Nicotinamide was found considerably more efficient than urea and induced a bathochromic shift of RF's absorption spectrum [30]. Classical molecular dynamics suggested π-stacking of RF with nicotinamide to be the reason for the bathochromic shift and for the increase in RF's water solubility [8,31,32]. However, the acceleration of the photodegradation of the anyway very photosensitive vitamin by nicotinamide from first to second order kinetics makes nicotinamide an inappropriate hydrotrope for RF [33].

Even without nicotinamide, RF is photodegraded within some hours upon exposure to sun light [29,34,35]. Additionally, photoexcited RF can photosensitize other compounds. As a consequence, the color, odor, and taste of products may be altered [36,37].

RF's water solubility is pH-dependent. Although RF is readily soluble in alkaline medium due to deprotonation of the hydroxy groups on the ribityl chain, the vitamin is degraded considerably faster at alkaline pH-values even in the dark and even more upon light exposure [34].

Hence, an optimal RF solubilizer should be non-toxic, should maintain a constantly neutral or acidic pH-value, and should not accelerate or, even better, should retard RF's photodegradation. Based on our last findings [25], such a hydrotrope should especially weaken π-stacked aggregation of RF in water.

Using RF as a solute, in this article, we investigate the solubilizing performance of a class of molecules as cheap natural hydrotropes. The latter are polyphenolic acid salts and derivatives.

### 1.3. Utilized hydrotropes – Investigation of the solubilizing mechanism

Polyphenolic acids were reported to undergo stacking with theobromine and caffeine, and molecular dynamic suggests π-stacking of salicylic acid and RF [38–41]. Moreover, some polyphenolic acids were

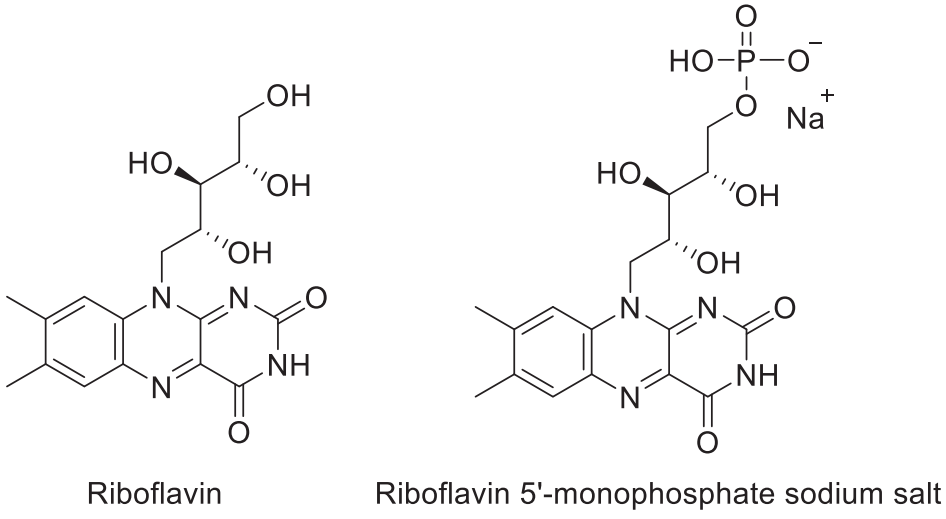


**Fig. 1.** Molecular structure of riboflavin (RF) and riboflavin 5′-monophosphate sodium salts (RF-$PO_4$).

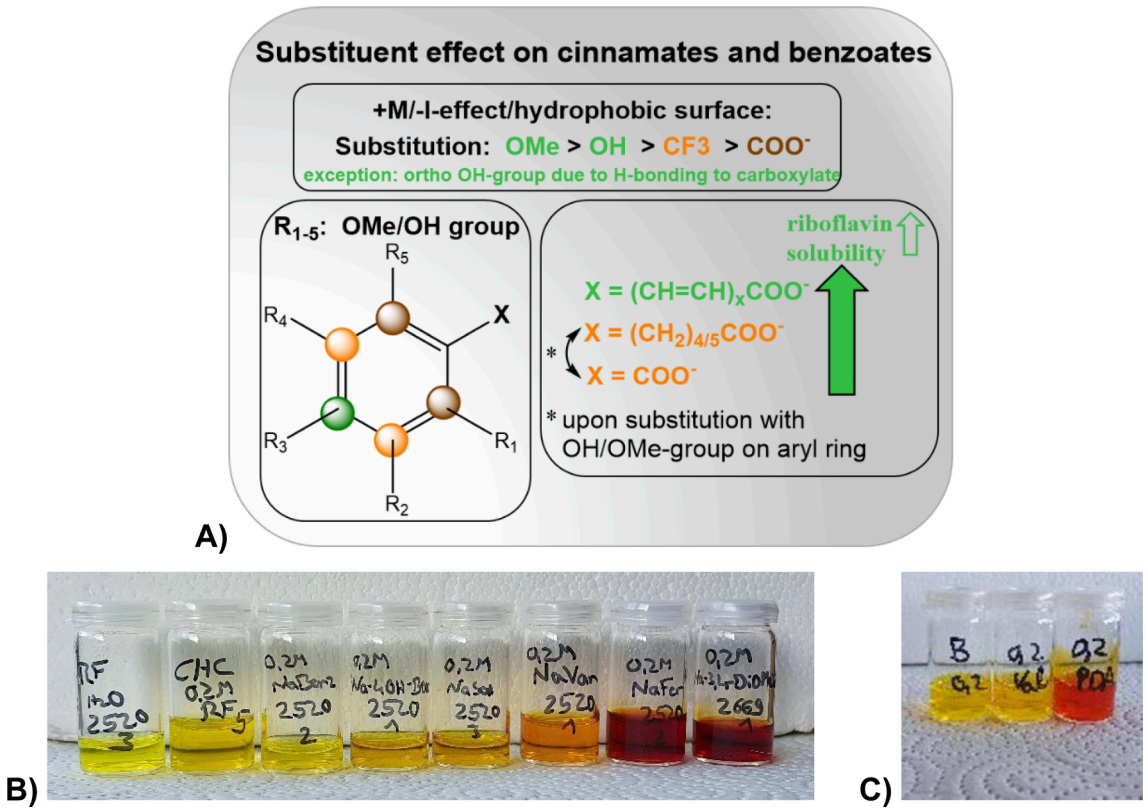


**Fig. 2.** (A) Effect of a functionalization of the aryl backbone, as present in natural sodium polyphenolates, on the riboflavin solubilizing power in water. The solubilization power increases from brown to orange and green. (B) From left to right: pure riboflavin in water (saturation) and with 0.2 mol·kg$^{-1}$ NaCHC, NaBenz, Na-4-OH-Benz, Na-2-OH-Benz, Na-4-OH-3-OMe-Benz, Na-4-OH-3-OMe-Cinn, Na-3,4-DiOMe-Cinn in water saturated with riboflavin. (C) From left to right: 0.2 M NaButyrate, 0.2 M NaValerate, 0.2 M Na-2,4-pentadienoate. From left to right, the solubilization efficiency of the additive increases in B and C. (For interpretation of the references to color in this figure legend, the reader is referred to the web version of this article.)

already shown to quench the photoexcited singlet and triplet state of RF [36,42]. The wide occurrence of polyphenolic acids in cereals, vegetables and fruits, and the application of benzoic acid derivatives by the flavoring industry make polyphenolic acids potential additives for food, beverage and pharma products [43–45]. However, the solubility of polyphenolic acids in water is low. Therefore, we decided to investigate the better water-soluble sodium polyphenolates as hydrotropes for RF [46]. Sodium was chosen, as it is the major cation in the extracellular fluid [47,48]. We focused mainly on the variation of the organic polyphenolate residue, because according to a patent, the variation of the cation from sodium (15.41 mmol·L$^{-1}$) to potassium (19.4 mmol·L$^{-1}$) increased the solubility of RF in presence of gallate only by 26 % [46].

To see the impact of an organic cation, some choline polyphenolates were also tested as solubilizers for RF. Choline was chosen, as it is an organic nutraceutical and because the corresponding polyphenolates are highly water-soluble. The high water solubility of choline polyphenolates was supposed to promote the water solubility of RF further [49,50].

The solubilizing power and efficiency of sodium/choline polyphenolates towards RF in water was analyzed via saturation experiments with a UV–Vis-spectrophotometer. To understand the solubilization mechanism, hydroxy-(OH), methoxy- (OMe) and even trifluoromethyl-substituted sodium benzoate and cinnamate derivatives, a salting-in/-out agent, a typical hydrotrope, and a surfactant were tested as solubilizing agents. The abbreviations of tested solubilizers are given in Fig. 3 in Section 3.2.1. To know if the solubilization of RF by means of sodium polyphenolates is based on aggregation, surface tension and dynamic light scattering (DLS) experiments of some aromatic sodium carboxylates in water were performed in the absence and presence of RF.

Concentration-dependent absorption spectra of RF and sodium ferulate at a constant molar ratio were recorded to see if the absorption spectrum of RF is altered due to a potential π-complexation. To understand the interactions better, one- and two-dimensional NMR measurements of RF and RF-$PO_4$ were performed in the absence and presence of aromatic sodium carboxylates. Finally, the solubilizing mechanism was investigated from a theoretical point of view via separation of the Coulomb electrostatic and the Lennard Jones potential energy, via cluster analysis of molecular dynamics (MD) simulations of RF in the presence of several aromatic sodium carboxylates. Separation energy of two RF molecules was quantified by umbrella sampling.

## 2. Experimental

### 2.1. Material

Deionized Millipore water (18 MΩ·cm) was taken from a Millipore purification system from Merck Millipore (Billerica, MA USA). Riboflavin (97 %) was purchased from Carl Roth (Karlsruhe, Germany). Riboflavin 5′-monophosphate sodium salt (73–79 %, <10.5 % $H_2O$; 3.8–6.5 % Na (anhydrous)), cinnamic acid (>99 %, FCC, FG), *trans*-ferulic acid (99 %), sodium benzoate (99 %, p.A.), sodium salicylate (99.5 %, reagent plus), sodium thiocyanate (99.99 %), sodium xylene sulfonate (<9.0 % sodium sulfate), 2,4,6-trihydroxybenzoic acid monohydrate (90 %, predominantly 1,3,5-benzenetriol), and tyrosol (>98.0 %) were purchased from Sigma Aldrich (Darmstadt, Germany). Gallic acid (98.0 %, for synthesis), 4-phenylbutyric acid (99 %), sodium dihydrogen phosphate dihydrate (pro analysis), and sodium dodecyl sulfate (99 %) were purchased from Merck (Darmstadt, Germany). 3,4-Dimethoxycinnamic acid (>98.0 %), caffeic acid (>98.0 %), cyclohexane carboxylic acid (>98.0 %), 2,3-dihydroxybenzoic acid (>98.0 %,

HPLC), 2,4-dihydroxybenzoic acid (>98.0 %, HPLC), 3,4-dihydroxybenzoic acid (>98.0 %), 3,5-dihydroxybenzoic acid (>98 %), 2,4-dimethoxybenzoic acid (>99 %), 2,3-dimethoxybenzoic acid (>98 %, GC), 3,4-dimethoxybenzoic acid (>98.0 %), 3,5-dimethoxybenzoic acid (>98.0 %, GC), 3-(4-hyroxyphenyl)propionic acid (98.0 %), p-anisic acid (>99.0 %, GC), o-anisic acid (>98.0 %, GC), p-coumaric acid (>98.0 %, HPLC), m-anisic acid (>98.0 %, GC), (2E,4E)-5-phenyl-2,4-pentadienoic acid (>98.0 %, GC), 5-phenylvaleric acid (>99.0 %), sinapinic acid (98.0 %, GC), sodium 4-hydroxybenzoate (98.0 %), sodium 3-hydroxybenzoate (99.0 %), sodium terephthalate (99.0 %, HPLC), sodium vanillate (98.0 %), syringic acid (97.0 %), *trans*-m-coumaric acid (>98.0 %, GC), *trans*-4-methoxycinnamic acid (>98.0 %, GC), and *trans*-o-coumaric acid (>98.0 %, GC) were purchased from TCI Chemicals (Eschborn, Germany). 3,5-Bis(trifluoromethyl)benzoic acid (98 %) was purchased from Thermo Scientific Fisher (Germany). Sodium hydroxide (p.A., Pellets, AnalaR Normapur) was purchased from VWR (Ismaning, Germany). Sodium ferulate (99.54 %) for NMR analysis was purchased from BDLpharm (Kaiserslautern, Germany). Deuterated dimethyl sulfoxide (99.8 %) and deuterium oxide (99.96 %) were purchased from Deutero (Kastellaun, Germany).

If not stated otherwise, all samples were prepared and measured at 23 °C in the dark.

### 2.2. Solubilization of riboflavin

The sample size was 1.5–2.5 g. For salt concentrations below 0.1 mol $kg^{-1}$, up to 10 g samples were prepared to gain more accuracy.

#### 2.2.1. Preparation of aqueous sodium salt and tyrosol samples with riboflavin

The samples were prepared via neutralization of the corresponding carboxylic acid with self-made sodium hydroxide solution. Samples comprising NaBenz, Na-2-OH-Benz, Na-3-OH-Benz, Na-4-OH-Benz, Na-4-OH-3-OMe-Benz, Naterephthalate, NaSCN, NaH2PO4, sodium dodecyl sulfate, sodium xylene sulfate, and tyrosol were prepared via direct dissolution of the compound in water. If the compound was not solubilized after stirring at 450 rpm for 1 h, the compound was regarded to be insoluble in water. To all samples, no matter if homogeneous or heterogeneous, RF was added in excess. The samples were ultrasonicated for 2 min (Bransonic 220, 120 W, frequency: 50 kc) and stirred at 450 rpm for 1 h. The samples were filtered through 0.45 μm polytetrafluoroethylene (PTFE) filters.

Samples comprising Na-2,4,6-TriOH-Benz, Na-2,4-pentadienoate, NaValerate, NaButyrate and tyrosol were prepared in triplicate. Samples comprising Na-4-OH-3,5-DiOMe-Cinn and NaH2PO4 were prepared once. The residual samples were prepared in duplicate. For the quantification of RF, see [25].

#### 2.2.2. Preparation of aqueous choline polyphenolate/cinnamate samples with riboflavin

Choline gallate, vanillate, 3,5-dihydroxybenzoate, ferulate, cinnamate or 3,4-dimethoxybenzoate solutions were prepared via neutralization of the corresponding carboxylic acid with aqueous choline hydroxide solution (46 wt%). After stirring at 450 rpm for 15 min, RF was added in excess. The samples were ultrasonicated for 2 min (Bransonic 220, 120 W, frequency: 50 kc) and stirred at 450 rpm for 1 h. After filtration through 0.45 μm PTFE filters, RF was quantified as detailed in [25]. The samples were prepared in duplicate.

### 2.3. Surface tension measurements

The surface tension curves were recorded with a Krüss (Hamburg, Germany) Tensiometer K100 at 25 °C by the Wilhelmy Ring Method (platinum-iridium-ring). For the surface tension curves of Na-4-OH-3-OMe-Cinn and NaCinn, stock solutions in water were prepared via neutralization of the corresponding acid with 1 M self-made sodium hydroxide solution and addition of the residual amount water. In the case of NaBenz and Na-2-OH-Benz, the sodium salt was directly dissolved in water. The stock solutions were saturated with RF and ultrasonicated for 2 min (Bransonic 220, 120 W, frequency: 50 kc). After stirring at 450 rpm for 1 h, surface tension curves were recorded as described in [51]. All samples were prepared twice.

### 2.4. Dynamic light scattering measurements

All samples were filtered into borosilicate tubes with 0.22 μm PTFE filters. With an ALV/CGS-3 goniometer (Langen, Germany) with an ALV/LSE-5004 correlator and with an ALV correlator software, DLS correlation functions of sodium polyphenolates and RF in pure water, and of sodium polyphenolate solutions saturated with RF were measured at 90° at 25 °C. A vertically polarized HeNe laser (22 mW, 632.8 nm) was used for the measurements. For more information on the method see Klossek et al. [52] All samples were prepared in triplicate.

#### 2.4.1. Sample preparation of aromatic sodium carboxylates in water

0.37 mol·$kg^{-1}$ aqueous sodium ferulate solutions were prepared via neutralization of the corresponding acid with 1 M self-made sodium hydroxide solution. Sodium benzoate and salicylate were dissolved directly in water at a concentration of 1 mol·$kg^{-1}$.

#### 2.4.2. Sample preparation of aqueous sodium polyphenolate solutions saturated with riboflavin

An excess of RF was added to the samples from section 2.4.1. The samples were ultrasonicated for 2 min (Bransonic 220, 120 W, frequency: 50 kc) and stirred at 450 rpm for 1 h. Additionally, 1 mol·$kg^{-1}$Na-3,4-DiOMe-Cinn samples were prepared via neutralization of the corresponding acid with 6 M self-made sodium hydroxide solution and saturation with RF as described above. As a reference sample, water was saturated with RF. All samples were filtered through 0.45 μm PTFE filters.

### 2.5. Nuclear magnetic resonance measurements

Proton Nuclear Magnetic Resonance ($^{1}$H NMR), 13-Carbon Nuclear Magnetic Resonance ($^{13}$C NMR), Correlation Spectroscopy (COSY), Heteronuclear Multiple Bond Correlation (HMBC) experiments, Heteronuclear Single Quantum Coherence (HSQC) experiments and NOESY (Nuclear Overhouser Spectroscopy) experiments were performed at a Bruker Avance III HD 400 (400.13 MHz) NMR-spectrometer with a 5 mm BBO 400SB BB-H-D or with a 5 mm BBO 400S1 BBF-H-D probe head with a Z-gradient at the Central Analytical NMR department of the University of Regensburg.

#### 2.5.1. NMR measurements in riboflavin/aromatic sodium carboxylate solutions

NMR experiments were performed in DMSO-$d_6$. Samples comprising RF and NaBenz, Na-3-OH-Benz, Na-4-OH-Benz, Na-4-OH-3-OMe-Benz and NaCinn were saturated with RF. For saturation of DMSO-$d_6$, an excess of the compounds was added to 1 g solvent. The samples were stirred for 1 h. In the case of NaCinn in presence of RF at the molar ratio 1, the sample was diluted with DMSO-$d_6$ after filtration through 0.45 μm PTFE filters and then again saturated with NaCinn. The following aromatic sodium carboxylate/RF samples were obtained: NaBenz/RF with the molar ratio 2, Na-3-OH-Benz/RF with the molar ratio 11, Na-4-OH-Benz with the molar ratio 2, Na-4-OH-3-OMe-Benz with the molar ratio 1, NaCinn/RF with the molar ratios 0.4 and 1.

To see if the chemical shift of RF and of the additives depends on the additive to RF ratio, four different Na-2-OH-Benz/RF molar ratios were prepared (Ratio 2: DMSO-$d_6$: 1.993 g, Na-2-OH-Benz: 0.009 g, RF: 0.010 g; Ratio 5: DMSO-$d_6$: 2.017 g, Na-2-OH-Benz: 0.024 g, RF: 0.011 g; Ratio 10: DMSO-$d_6$: 1.966 g, Na-2-OH-Benz: 0.113 g, RF: 0.026 g; Ratio 50: DMSO-$d_6$: 3.012 g, Na-2-OH-Benz: 0.243 g, RF: 0.011 g). The

samples were stirred at 450 rpm until dissolution.

Reference samples of all sodium salts were prepared via saturation of DMSO-$d_6$ with the compounds. After filtration through 0.45 μm PTFE filters, all samples (0.8 mL) were filled into NMR tubes.

For a NOESY measurement, 3.0 mol·kg$^{-1}$ Na-3,4-DiOMe-Cinn in water was saturated with RF via ultrasonication for 2 min (Bransonic 220, 120 W, frequency: 50 kc) and stirring at 450 rpm for 1 h. After filtration through 0.45 μm PTFE filters, the sample (0.8 mL) was filled into an NMR tube.

#### 2.5.2. NMR measurements in riboflavin phosphate sodium salt/sodium ferulate solution

To obtain a maximum resolution, deuterium oxide was saturated with sodium ferulate and RF-$PO_4$ via stirring at 450 rpm for 1 h. After filtration through 0.45 μm PTFE filters, 0.8 mL of the sample was filled into the NMR tube. For $^{13}$C NMR measurements, an insert with DMSO-$d_6$ was inserted to have a reference peak.

### 2.6. Computational details

MD simulations were performed with GROMACS version 2022 [53–60]. The TIP4P water model was used. The GAFF force field [61,62] was used employing ACPYPE for the generation of the parameters [63]. RESP charges [64] were derived after geometry optimization for RF and all aromatic carboxylates in the gas-phase at the M062X/def2-TZVP [65–67] level of theory. The quantum chemical calculations were done using ORCA 5.0.3 [68] employing the RICOSX [69] approximation. The effect of additives in the solubilization of RF in water was studied by molecular dynamics simulations of RF molecules with a molar ratio of 1:10 with respect to various sodium polyphenolates in water. Similar to our previous study in pure water [25], 8 RF molecules in a ~ 512 nm$^3$ cubic box with 80 polyphenolate molecules (charges neutralized with equimolar of sodium ion) were simulated at 300 K in the NPT ensemble using a Bussi thermostat and barostat [70,71] Umbrella sampling was carried out to estimate the separation free energy of 2 RF molecules in the presence of sodium ferulate. In this case, 20 ferulate molecules were included in the 4x8x4 nm$^3$ water box. To generate the initial configuration, pulling of RF molecule was performed at a rate of 1 nm·ns$^{-1}$ with a force constant of 1000 kJ mol$^{-1}$·nm$^{-2}$. NPT equilibrations of 200 ns were preceded by 100 ps of NVT equilibration. The NPT equilibrations were done for each sampling window. Mostly, a force constant of 1000 kJ mol$^{-1}$ nm$^{-2}$ was applied in the sampling phase. For the configuration with center of mass-distance (COM) of 0.54 nm between two RF molecules, the force constant was doubled to achieve better sampling at this separation distance. Finally, the free energy profile was obtained by the weighted histogram analysis method, WHAM [72] (the first 25 ns were discarded, see Fig. A 86 for the histogram). Additionally, dissociation enthalpy and entropy were calculated for the system in pure water and in the system with additive. This was realized by averaging of the potential energy using a binning procedure according to the COM separation distance.

## 3. Results and discussion

### 3.1. Solubilization of riboflavin by sodium polyphenolates

Based on the findings of a US-Patent from 1946, we studied the effect of polyphenolates on RF's water solubility with UV–Vis-spectroscopy [46]. To exclude pH contributions to RF's water solubility, the pH-value of all samples was controlled with indicator paper to be constantly 7. For the exact water solubility of RF in the presence of the additives see section 8.3 in the Supplementary Material.

As expected, sodium polyphenolates turned out to be good hydrotropes for RF. RF's solubility was increased exponentially with sodium polyphenolate concentration, see section 8.1 in Supplementary Material. Among the polyphenolates tested, Na-4-OH-3-OMe-Cinn, Na-3,4-DiOMe-Cinn, Na-4-OH-3,5-DiOMe-Cinn, and Na-2,4,6-TriOH-Benz increased riboflavin's solubility most efficiently (low molar polyphenolate/RF ratio), see Table 1 left and sections 8.1 and 8.3 in Supplementary Material. The most efficient sodium polyphenolates, Na-3,4-DiOMe-Cinn, Na-4-OH-3,5-DiOMe-Cinn, Na-4-OH-3-OMe-Cinn and Na-2,4,6-TriOH-Benz increased the water solubility of RF > 2000 times, >1400 times, >240 times and >65 times at the highest tested additive concentration of 4.34 mol·kg$^{-1}$, 1.62 mol·kg$^{-1}$, 0.56 mol·kg$^{-1}$, and 0.08 mol·kg$^{-1}$, respectively, see Table 1 right. (Na-4-OH-3,5-DiOMe-Cinn and Na-2,4,6-TriOH-Benz might be even more efficient, but were not tested at higher additive concentrations due to cost and toxicological reasons, respectively. For Na-3,4-DiOMe-Cinn, the solubilization was not continued above 4.34 mol·kg$^{-1}$, as the stirring and filtering process was impeded due to high viscosity.)

A comparison of polyphenolates with the common hydrotrope sodium xylene sulfonate (SXS) showed that Na-4-OH-3,5-DiOMe-Cinn at 1.62 mol·kg$^{-1}$ and Na-3,4-DiOMe-Cinn at 1.73 mol·kg$^{-1}$ were > 17 times and 13 times more efficient RF solubilizers than SXS at ≈ 1.9 mol·kg$^{-1}$, respectively. The typical salting-in agent NaSCN was also worse than all tested sodium polyphenolates, see Fig. A 7 in section 8.1. Even the standard surfactant sodium dodecyl sulfate (SDS) (0.4 mol·kg$^{-1}$) solubilized > 14 times less RF than the RF solubilizers Na-4-OH-3,5-DiOMe-Cinn, Na-3,4-DiOMe-Cinn and Na-4-OH-3-OMe-Cinn at the same concentration, respectively. Moreover, at an additive concentration of 1 mol·kg$^{-1}$, Na-4-OH-3,5-DiOMeCinn and Na-3,4-DiOMe-Cinn solubilized respectively >72 and >55 times more RF than the common RF solubilizer nicotinamide [30]. Regarding a patent, which presents sodium gallate as potent RF solubilizer for pharmaceutical application, Na-4-OH-3,5-DiOMe-Cinn and Na-3,4-DiOMe-Cinn solubilized 4.15 times and 2.9 times more RF than sodium gallate at 0.67 mol·kg$^{-1}$ (corresponding to the solubility of sodium gallate in presence of RF due to the mutual increase in solubility of RF and gallate). In the presence of RF, even sodium ferulate solubilized 1.8 times more RF at its solubility limit (0.56 mol·kg$^{-1}$) than sodium gallate at its solubility limit (0.67 mol·kg$^{-1}$). Consequently, the majority of the tested sodium polyphenolates exhibits a solubilization efficiency considerably superior to the one of a common salting-in agent, hydrotrope, surfactant and even superior to the one of the common RF solubilizers nicotinamide and Na-3,4,5-TriOH-Benz [30].

Using UV–Vis-measurements, choline polyphenolates were also tested as solubilizers for RF to see if the extraordinary hydrotropic action of sodium polyphenolates is linked to the nature of the cation [46]. As for the sodium salts, the water solubility of RF was increased exponentially with the choline polyphenolate concentration, see section 8.2 in Supplementary Material. Choline and sodium polyphenolates exhibited similar solubilizing properties for salt concentrations <0.6 mol·kg$^{-1}$. Yet, the sodium salts have a limited solubility and thus the better water-soluble choline salts led to a greater absolute enhancement of the aqueous solubility of RF, see Fig. A 9 in Supplementary Material. Nevertheless, lower molar polyphenolate/RF ratios and thus greater solubilizing efficiencies were achieved with sodium polyphenolates

**Table 1**
Best molar polyphenolate/riboflavin ratio obtained with the most efficient sodium polyphenolates and maximum water solubility of riboflavin in the aqueous solubilization of riboflavin at the given additive concentration.

| Additive | Ratio (additive/riboflavin) | Solubility of riboflavin |
|---|---|---|
| **Na-2,4,6-TriOH-Benz** | **4.5** at 0.08 mol·kg$^{-1}$ | **18 ± 1 mmol·kg$^{-1}$** at 0.08 mol·kg$^{-1}$ |
| **Na-4-OH-3,5-DiOMe-Cinn** | **4.2** at 1.02 mol·kg$^{-1}$ | **380 mmol·kg$^{-1}$** at 1.62 mol·kg$^{-1}$ |
| **Na-3,4-DiOMe-Cinn** | **5.8** at 1.09 mol·kg$^{-1}$ | **560 ± 20 mmol·kg$^{-1}$** at 4.34 mol·kg$^{-1}$ |
| **Na-4-OH-3-OMe-Cinn** | **6.3** at 0.37 mol·kg$^{-1}$ | **67 ± 2 mmol·kg$^{-1}$** at 0.56 mol·kg$^{-1}$ |

(except of gallate). Consequently, if a low solubilizer/RF ratio and a neutral odor is required, sodium salts are more appropriate. As the usage of choline polyphenolates combines a vitamin with two nutraceuticals – polyphenolates and choline, choline polyphenolates might be advantageous RF solubilizers for dietary supplements [49].

### 3.2. Solubilizing mechanism

#### 3.2.1. Insights from solubilization tests

The solubilization mechanism of the system RF/polyphenolate/water was analyzed with various sodium carboxylates, with a salting-in/-out agent, a common hydrotrope, and a surfactant. A summary of the trends will be given in this section. For more details see Section 8.1 in the Supplementary Material. A ranking of the efficiency of all hydrotropes tested is given in Fig. 3.

RF's water solubility increased with the size of the polyphenolate's hydrophobic moiety, which correlates with the solubilizers' amphiphilicity and would be decisive for an aggregative solubilization of RF. However, the conjugated π-electron system was significantly more dominant in RF's aqueous solubilization. The larger the conjugated electronic system of the solubilizer, the more RF was solubilized in water. Functionalization of the aryl ring with hydroxy and methoxy groups improved the solubilizing efficiency more with greater distance of the functional group from the carboxylate (para > meta > ortho). For the solubilization of RF, amphiphilicity was not as crucial as a functionalization of the solubilizer with a group exhibiting a positive mesomeric and lower minus inductive effect (Na-3,4,5-TriOH-Benz > NaBenz; OMe > OH > $CF_3$ > $COO^-$). The effect of functionalization of the aryl ring on the solubilizing power of the aromatic sodium carboxylates is visualized in Fig. 2 A.

A concentration-dependent bathochromic shift of RF's absorption spectrum was observed in the presence of high concentrations of "electron richer" aromatic sodium carboxylates (>0.1 mol·kg$^{-1}$), see Fig. 2 B and Fig. A 8 in Supplementary Material. The sample's color did not change upon variation of the hydrophobic chain length (NaButyrate → NaValerate), but upon enlargement of the conjugated electronic system (NaValerate → Na-2,4-pentadienoate), see Fig. 2 C. A variation of the sample's coloration depending on the aromatic system of the solute and solubilizer is typical of HOMO-LUMO interactions in π-stacked molecular assemblies [73].

Additionally, mutual solubilization of RF and many aromatic sodium carboxylates was observed. Hence, RF even increased the water solubility of the scarcely water-soluble Na-3,4-DiOMe-Cinn, Na-4-OH-3,5-DiOMe-Cinn and Na-4-OMe-Cinn.

Moreover, water-insoluble aromatic sodium carboxylates solubilized RF occasionally more efficiently than soluble ones. For instance, the insoluble Na-3,4-DiOMe-Cinn solubilized 25.7 times more RF in water than the well water-soluble NaBenz at 1 mol·kg$^{-1}$ of the hydrotropes.

Hence, the solubilization properties of sodium polyphenolates do not correlate with the sodium polyphenolate's water solubility.

Main observations regarding RF's hydrotropic solubilization by sodium polyphenolates, related compounds and other solubilizers are summarized in Table 2. These are categorized as arguments for/against aggregation of sodium polyphenolates in the surrounding of RF, as arguments for/against hydration of RF by means of the additives, and as arguments for/against π-stacking based solubilization of RF as driving force in the hydrotropic solubilization of RF by sodium polyphenolates.

From the solubilization tests, we concluded π-complexation of RF and aromatic sodium carboxylates as driving force for the strong hydrotropic action of polyphenolates. This was affirmed by the similar hydrotropic solubilization of lumichrome by aromatic sodium carboxylates, which was also accompanied by a bathochromic effect. As the relative improvement of RF's and lumichrome's water solubility was almost identical, primary, the isoalloxazine ring is essential for the

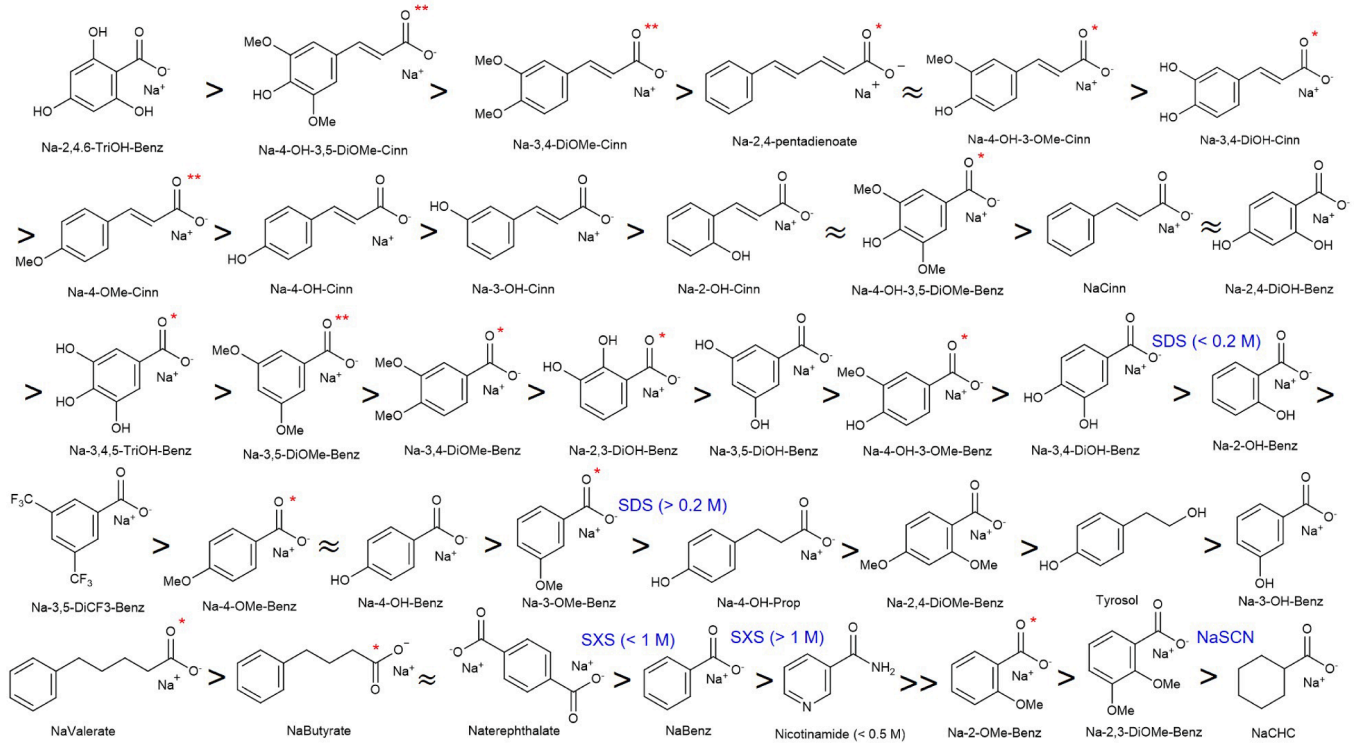


**Fig. 3.** Riboflavin solubilizers ordered according to their solubilizing efficiency (molar solubilizer/riboflavin ratio). Sometimes the slope of the solubilization curves (=molar solubilizer/RF ratio) changed with the solubilizer's concentration. Then the solubilization efficiency was regarded above 0.2 mol·kg$^{-1}$ of the additive concentration. *Riboflavin further increased the water solubility of the compound. **Not only the compound itself solubilized riboflavin, but riboflavin solubilized the totally insoluble compound in water, too. The corresponding solubilization curves and trends are displayed and explained in section 8.1 in Supplementary Material. Nicotinamide: [30]; M = mol·kg$^{-1}$.

**Table 2**
Pro (↑) and contra (↓) arguments for a solubilization of riboflavin (RF) in water with sodium polyphenolates via aggregation, π-stacking and hydration as main solubilization mechanism. Minimum hydrotrope concentration (MHC), critical aggregation concentration (CAC), sodium xylene sulfonate (SXS), sodium dodecyl sulfate (SDS), for further abbreviations, see Fig. 3.

| Aggregation | π-stacking | Hydration |
|---|---|---|
| ↑Polyphenolate backbone is amphiphilic.<br>↑All sodium cinnamates > sodium benzoates. | ↑All sodium cinnamates > sodium benzoates. | ↑ Salting-in/out agent in-/decrease the solubility of RF (NaSCN/NaH2PO4). |
| ↑After reaching a critical polyphenolate concentration (maximum of the additive/RF ratio), the solubilizing efficiency improves considerably. → might correspond to an MHC. | ↓No break point in the log–log-plot, see Fig. A 1, C, and D<br>↓Theoretical MHC region obtained from the maximal additive/RF ratio at polyphenolate concentrations <0.21 $mol \cdot kg^{-1}$, but typical CACs of benzoates/cinnamates are >0.2 $mol \cdot kg^{-1}$. [51] | |
| ↑Dependence on the hydrophobic chain length (SDS > NaValerate > NaButyrate > NaBenz). | ↑Weak dependence on the hydrophobic chain length (NaButyrate → NaValerate: +29 %). | |
| | ↑Deterioration of amphiphilicity improves solubility of RF (Na-3,4,5-TriOH-Benz > NaBenz).<br>↑Solubility increases with increasing + M and decreasing −I-effect (OMe > OH > CF3 > $COO^-$).<br>↑Increase of conjugated electron system improves solubility (Na-4-OH-3-OMe-Cinn ≈ Na-2,4-pentadienonate ≫ NaValerate; Na-4-OH-Cinn ≫ Na-4-OH-Benz > Na-4-OH-Prop).<br>↑Induction of conjugation improves solubility (NaBenz ≫ NaCHC).<br>↑Electronegative substituent in the aromatic ring lowers solubility (Nicotinamide < NaBenz).<br>↑Even without a carboxylate group, tyrosol solubilized RF →aromaticity sufficient for a solubilization.<br>↑Red-shift of RF's absorption spectrum for high concentrated sodium polyphenolate/RF solutions<br>↑Red-shift upon induction of a conjugation (NaValerate → Na-2,4-pentadienoate)<br>↑Mutual solubilization of RF and sodium polyphenolates.→ Copigmentation | ↑The solubility of RF rises with increasing number of OH-groups.<br>↑para > meta > ortho substitution with OH– and OMe- groups (except Na-2-OH-Benz).<br>↑Compounds with non-neighbored OH/OMe-groups are better solubilizers than the ones with adjacent groups.<br>↓OMe > OH on the aryl ring, although OMe more lipophilic.<br>↑Hydratable carboxylate improves solubility of RF (Tyrosol < Na-4-OH-Benz).<br>↓Totally insoluble compounds Na-3,4-DiOMe-Cinn and Na-4-OH-3,5-DiOMe-Cinn are more efficient solubilizers than water-soluble NaBenz, Na-2-OH-Benz and Na-3,4,5-TriOH-Benz.<br>↑In spite of lipophilic methyl groups, SXS with its less hydrated sulfonate group is a solubilizer comparable to NaBenz. [12]<br>↓Mutual solubilization.<br>↓Mutual solubilization even with totally insoluble sodium polyphenolates. |

hydrotropic effect of aromatic sodium carboxylates on RF [74]. Apparently, in water, this π-complex exhibits an improved hydration compared to the separate biomolecules. Otherwise, RF would not solubilize its solubilizer. Due to their mutual solubilization, one can consider RF and some polyphenolates as their mutual "co-hydrotropes". As the absorption spectrum/yellow coloration of RF can be regained upon dilution of the solutions with water, the interactions of RF and polyphenolates are probably rather weak and reversible. The regain of yellow coloration upon dilution with water confirms even more the assumption of complex formation between RF and polyphenolates.

### 3.2.2. Insights from NMR measurements

NMR measurements were conducted with DMSO-$d_6$, due to poor solubility of RF in other NMR solvents. The samples were prepared via saturation of DMSO-$d_6$ with RF and/or aromatic sodium carboxylates to have a sufficient signal to noise ratio. Hence, all samples exhibited a distinct molar carboxylate/RF ratio. The spectrum of RF in pure DMSO-$d_6$ is reported in [25]. Additionally, the dependence of the chemical shift Δδ of RF's and salicylate's protons/carbons on the molar Na-2-OH-Benz/RF ratio was analyzed, see section 8.5.1.2 in Supplementary Material.

However, DMSO might suppress inter- and intramolecular interactions [75]. As the solubilization mechanism of RF by sodium polyphenolates is mainly based on the interaction of the aromatic rings, the RF analogue RF-$PO_4$ was used to further evaluate the interactions of RF with sodium polyphenolates in water. Therefore, NMR measurements of RF-$PO_4$ in the absence and presence of sodium ferulate were conducted in deuterium oxide, see section 8.5.1.7 in Supplementary Material and [25].

For RF, RF-$PO_4$, and for aromatic sodium carboxylates, the change of the protons'/carbons' chemical shift was analyzed, relatively to the pure compounds. Additionally, the cross-peaks in the NOESY spectrum of RF or RF-$PO_4$ in the presence of aromatic sodium carboxylates were used to evaluate the polyphenolate/RF interactions, see Section 8.5.1 in Supplementary Material.

Conclusions from NMR measurements are summarized below. A detailed discussion of the observations is reported in the Sections 8.5.1, 8.5.2, and 8.5.3 in the Supplementary Material.

### 3.2.3. Indications for π-stacking

In the presence of aromatic sodium carboxylates, indications for stacking of RF with other RF molecules were not found, see section 8.5 in Supplementary Material. However, the signal intensity of RF was poor, and DMSO-$d_6$ might reduce aggregation of RF compared to water. Therefore, it was necessary to conduct NMR measurements of the flavin in deuterium oxide, which was done with RF-$PO_4$. The NOESY spectrum of the RF-$PO_4$ in the presence of sodium ferulate (cross-peak of H3 with H8 and *H*10 of RF-$PO_4$) indicated stacking in anti-alignment of RF-$PO_4$ with other RF-$PO_4$ molecules in deuterium oxide, see Fig. A 30 and Fig. A 33B in the Supplementary Material. This is in line with our last research, where we concluded anti-stacked aggregation of RF and RF-$PO_4$ in aqueous solutions via NOESY measurements and molecular dynamics [25]. Presumably, polyphenolates cannot prevent self-stacking of RF-$PO_4$ totally. As the interaction surface between polyphenolates with RF and RF-$PO_4$ is the same, we suppose that RF also still stacks with other RF molecules in the presence of aromatic sodium carboxylates in water. This is in line with the results from cluster analysis in Section 3.2.3, which proposed only a reduction of the average RF cluster size.

Further, RF and aromatic sodium carboxylates induced a shift of almost all of each other's protons and carbons, see Fig. A 31 in Supplementary Material. In line with this, RF-$PO_4$ and sodium ferulate also changed the chemical shift of each other's protons/carbons in deuterium oxide, see Fig. A 29 in Supplementary Material. Hence, the entire carbon backbone and almost all protons are affected by the interactions of RF or RF-$PO_4$ with aromatic sodium carboxylates.

Also in line with the higher RF solubilizing efficiency of polyphenolates substituted with OMe-/OH-groups on the para position compared to the meta and this compared to the ortho position, the change of the chemical shift of NaBenz's, Na-3-OH-Benz's and Na-4-OH-Benz's carbon atoms increased from ortho to para position, see sections

8.5.1.1, 8.5.1.3 and 8.5.1.4 in Supplementary Material. Similarly, the change of the electro-magnetic environment of sodium vanillate's carbon next to the OMe-group correlates with the strong effect of OMe-groups on the RF solubilizing power of polyphenolates, see Fig. A 26 in Supplementary Material. These two observations correlate with the dependence of the polyphenolates' electronic π-system on their solubilizing efficiency.

The linear increase of the chemical shift of RF's and Na-2-OH-Benz's protons and carbons with the molar Na-2-OH-Benz/RF ratio exhibited a break point at ratios 10 and 5, respectively, see section 8.5.1.2 in Supplementary Material. If π-complexes of RF and Na-2-OH-Benz are formed in DMSO-$d_6$, the break point might correspond to a critical concentration for complexation of RF and Na-2-OH-Benz. Then, the two different ratios at which the break point occurred can be explained with the three times smaller size of Na-2-OH-Benz compared to RF.

As Na-3,4-DiOMe-Cinn underwent an extraordinary mutual solubilization with RF in water, a sufficiently intense NOESY spectrum of a 3.0 mol·kg$^{-1}$ Na-3,4-DiOMe-Cinn solution saturated with RF in water could be recorded to estimate the distance of the two biomolecules in solution.

Several cross-peaks between Na-3,4-DiOMe-Cinn's and RF's protons in the NOESY spectrum show that the polyphenolate and RF are close. As NOESY has a detection limit of 5 Å and common distances for π-stacked compounds are 3.46–3.85 Å, the proximity of RF's and Na-3,4-DiOMe-Cinn's protons along the entire molecules is in favor of π-stacked arrangement of RF and Na-3,4-DiOMe-Cinn, see Fig. 4 [76–80].

### 3.2.4. Indications for mutual hydration of RF and sodium polyphenolates

Peak broadening, loss of the splitting, deshielding of exchangeable protons and the presence of cross-peaks of exchangeable protons of RF-$PO_4$, RF, and aromatic sodium carboxylates with water proofed mutual hydration of RF and sodium polyphenolates, see section 8.5.1 in Supplementary Material. DMSO-$d_6$ always contains traces of water, which were attracted by RF and aromatic sodium carboxylates when being dissolved together. This observation is in line with the mutual solubilization of RF and some aromatic sodium carboxylates from Section 3.2.1.

Analogously, the attraction of sodium ferulate induced a stronger hydration of RF-$PO_4$. Thus, the cross-peak of the aromatic proton H2 of RF-$PO_4$ with water in the presence of ferulate was not present in the NOESY NMR spectrum of RF-$PO_4$ in pure deuterium oxide, see Fig. A 30b in Supplementary Material and [25]. Moreover, the degree of RF's hydration depended on the solubilizer/RF ratio, as with increasing molar Na-2-OH-Benz/RF ratio, the deshielding and peak broadening and thus the degree of deprotonation increased, see Fig. A 16B in Supplementary Material.

### 3.2.5. Conformation of the ribityl (phosphate) chain

Cross-peaks in the NOESY spectrum of RF in the presence of Na-2-OH-Benz, Na-4-OH-3-OMe-Benz and Na-3-OH-Benz pointed to an in average curved ribityl side chain conformation, see Fig. A 32 in Supplementary Material. Similarly, a cross-peak of RF-$PO_4$'s aromatic proton H2 with *H*11 and H12 on RF-$PO_4$'s ribityl phosphate chain pointed to a curved average ribityl phosphate chain in the presence of sodium ferulate, see Fig. A 30 and Fig. A 33 in Supplementary Material. In line with this, NPT simulations indicated a more rigid and curved ribityl chain conformation in presence of a polyphenolate, see Fig. A 87 in Supplementary Material.

While we suggested a curved ribityl chain of RF-$PO_4$ in water in our last publication, we supposed, based on COSMO-RS calculations, molecular dynamics, and NOESY experiments, RF's ribityl chain to be rather stretched and dynamic in pure water or DMSO-$d_6$ [25]. Therefore, we suppose that polyphenolates induce a change in the ribityl chain conformation. According to our last article, RF comprising a curved ribityl chain, should be better water-soluble than RF with a stretched one. Therefore, the sugar chain of RF-$PO_4$ might be already curved in

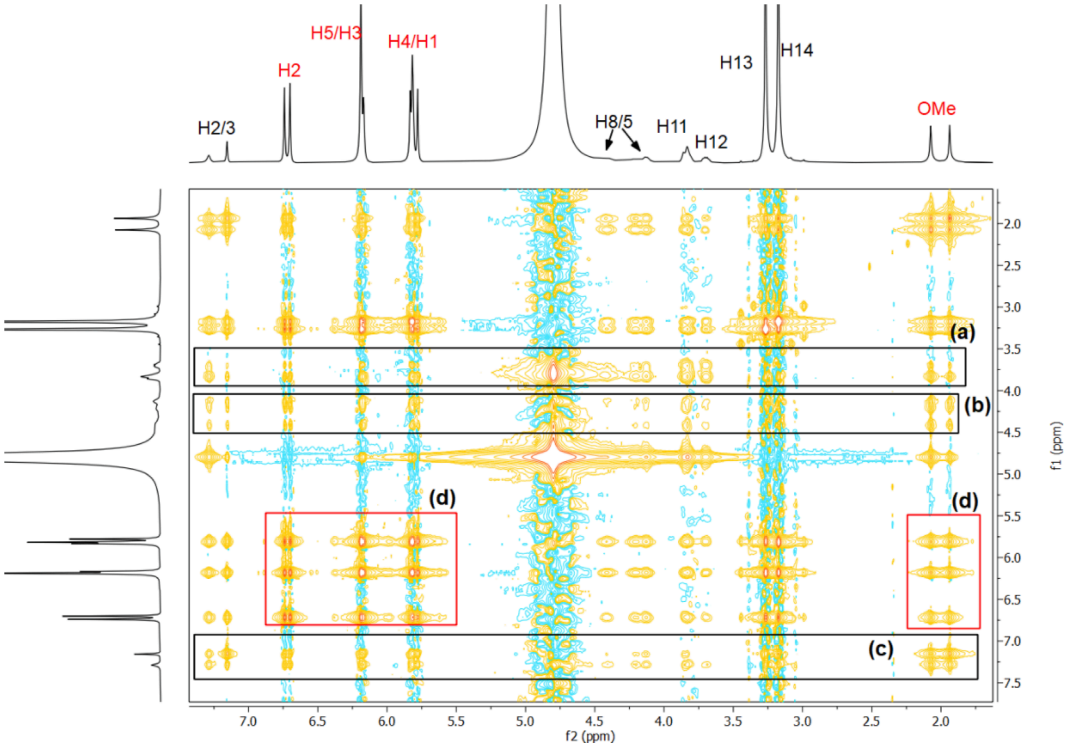


**Fig. 4.** NOESY spectrum of an aqueous 3 mol·kg$^{-1}$ sodium 3,4-dimethoxycinnamate solution saturated with riboflavin. (a) Cross-peaks of the ribityl chain protons H12 and *H*11 with H5/8, H2/3, H13/14 of RF and with H2, H5, H3, H4, H1 and with the methoxy groups of sodium 3,4-dimethoxycinnamate; (b) Cross-peaks of H8/5 of riboflavin with *H*11, H12, H2/3, H13/14 of RF and with H2, H5, H3, H4, H1 and with the methoxy groups of sodium 3,4-dimethoxycinnamate; (c) Cross-peaks of the aromatic protons H2/3 of RF with H13/14, *H*11, H12, H8/5 of RF and with H2, H3 H5, H4, H1 and with the methoxy groups of sodium 3,4-dimethoxycinnamate; (d) all protons of Na-3,4-DiOMe-Cinn interact with each other.

pure water, because the phosphate group induces strong hydration.

Besides, NOESY cross-peaks of NaBenz's aromatic protons H1 and H2 with RF's proton *H*11 on the ribityl side chain and the NOESY cross-peak of sodium ferulate's methoxy group with the ribityl chain protons *H*11/H12 of RF-$PO_4$ point to proximity of aromatic sodium carboxylates to RF's/RF-$PO_4$'s ribityl chain, c.f., Fig. A 15 and Fig. A 33 in Supplementary Material. Supposing stacking of RF/RF-$PO_4$ and aromatic sodium carboxylates, this proximity to the ribityl chain protons hints to a curved ribityl chain. Thus, stacking of aromatic sodium carboxylates with RF/RF-$PO_4$ might even alter the average ribityl chain conformation and lead to the mutual solubilization of RF and aromatic sodium carboxylates.

As the chemical shift of the protons/carbons of RF/RF-$PO_4$ and aromatic sodium carboxylates was minorly influenced by aromatic sodium carboxylates and RF/RF-$PO_4$, respectively, the interaction of RF with sodium polyphenolates seems rather weak, see section 8.5.1 in Supplementary Material.

### 3.2.6. Theoretical calculations

Simulation of RF molecules in water has shown firmly stacked aggregates formed and held together presumably by dispersive interaction due to the extended planar aromatic surface of RF. Using rigorous umbrella sampling, we estimated that the dissociation free energy is as high as 22 kJ·mol$^{-1}$ at room temperature. While structural properties of the aggregates suggest that π-π-interaction is predominating, separation of the non-covalent interaction in a highly complex system remains a challenging task in theoretical studies.

In this regard, the simple functional form of classical nonpolarizable force fields (given well-fitted parameter) provides a straightforward way to separate the non-bonded interaction energies. Eqs. (1)–(3) describe the non-bonded terms consisting of the Coulomb electrostatic term ($E_{Coulomb}$) and the Lennard Jones-potential term ($E_{LJ}$), which are calculated between a pair of particles *ij* in the force field simulation. The attractive term ($C_{ij}^{(6)}$) in the Lennard-Jones potential in molecular mechanics simulation can be turned off leaving the electrostatic term and the repulsive term active in the non-bonded interaction term (Eq. (4)). On the other hand, the electrostatic term can be deactivated by setting the charges $q_i$ to zero, and the non-bonded interaction is then simply comprised of pure LJ-term (Eq. (5)).

$$E_{\text{non-bonded}} = E_{Coulomb} + E_{LJ} \tag{1}$$

$$E_{LJ} = \frac{C_{ij}^{(12)}}{r_{ij}^{12}} - \frac{C_{ij}^{(6)}}{r_{ij}^{6}} \tag{2}$$

$$E_{Coulomb} = f\frac{q_i q_j}{r_{ij}} \tag{3}$$

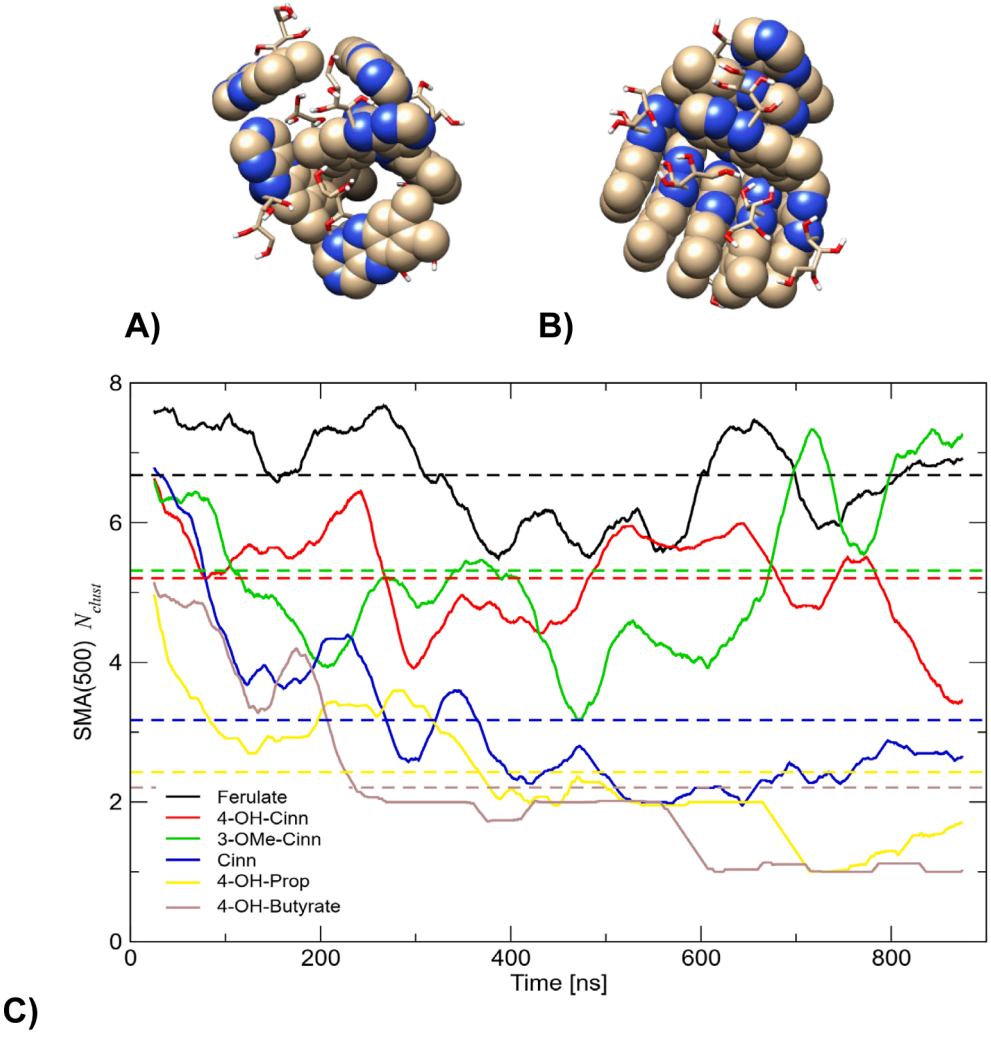


**Fig. 5.** Different stable aggregates of RF molecules formed when, A) Cij(6) = 0 and qi ≠ 0, B) Cij(6) ≠ 0 and qi = 0.) Simple moving average (SMA) over 500 data points of number of clusters $N_{clust}$ (900 ns NPT simulation) for riboflavin aggregates in the presence of sodium Ferulate = 6.68, Na-4-OH-Cinn = 5.20, Na-3-OMe-Cinn = 5.31, NaCinn = 3.17, Na-4-OH-Prop = 2.43, Na-4-OH-Butyrate = 2.21. Dashed lines represent the overall average of $N_{clust}$.

$$E^{C12+Q}_{\text{non-bonded}} = f\frac{q_i q_j}{r_{ij}} + \frac{C^{(12)}_{ij}}{r^{12}_{ij}} \tag{4}$$

$$E^{C12+C6}_{\text{non-bonded}} = 0 + \frac{C^{(12)}_{ij}}{r^{12}_{ij}} - \frac{C^{(6)}_{ij}}{r^{6}_{ij}} = E_{LJ} \tag{5}$$

This approach permits us to study the conformational changes or preferences of RF molecules in water induced by electrostatic or dispersive interaction. The MD simulations revealed that stable aggregates of RF are formed both when the electrostatic part and when the attractive Lennard-Jones part of the RF interactions are turned off, see Fig. 5 A, B. A remarkable difference, however, is recognizable. While stacked aggregate (as in the previous case) was observed when $C^{(6)}_{ij}$ is non-zero and $q_i$ is zero, the aggregate formed with zero $C^{(6)}_{ij}$ and non-zero $q_i$ seems to be rather stabilized by hydrogen (H)-bonds. Indeed, H-bond analysis showed clearly that only 0.865 HB was formed during 100 ns simulation in pure-LJ system. In contrast, 1.860 HB was predicted in the C12 + Q-system. These results demonstrate that stacked aggregates in our system are predominantly triggered by the attractive term of the LJ-potential.

This unfavorable dissociation energy due to the attractive π-π interaction contributes significantly to the insolubility of RF-molecules in water. Obviously, to increase RF's solubility in water, the dispersive interaction between RF must be disrupted. Addition of various aromatic sodium carboxylates to the solution has been shown experimentally to increase the RF's solubility in water.

The aromaticity of the aromatic sodium carboxylates was certainly decisive for RF's solubilization. Experimentally, a distinction of the electron richness and planarity of the solubilizer could not be realized in this system. To still evaluate the influence of the planarity and electron density of aromatic sodium carboxylates on RF's water solubility, cluster analysis of the MD simulations over 900 ns of 8 RF molecules in the presence of various polyphenolate(−like) molecules was performed. RF, with the chemical formula $C_{17}H_{20}N_4O_6$, consists of 47 atoms. Since 8 RF molecules are set in a simulation box, 376 atoms are inside the box. The analysis tool provided by Gromacs [53–60] was employed to calculate the aggregate size $N_{agg}$. The routine implemented in the analysis tool calculates the number of atoms in the defined cutoff from one reference atom at one time. Hence, if only „intermolecular contact" between the atoms of the RF molecules is counted, it will yield the average number of atoms of the „aggregates" in the system. This is the most straightforward way to calculate the average size of aggregation $N_{agg}$ at one time frame. Apart from $N_{agg}$, the analysis tool also provides the number of clusters $N_{clust}$ present at a given time.

The average size of the aggregates at one time frame for our system with 8 RF molecules ($N_{agg}$) is extracted from the MD trajectory and is defined by Eq. (6).

$$N_{agg} = \frac{376}{\sum N_n} = \frac{N_1 \cdot 47 + N_2 \cdot 94 + \cdots + N_8 \cdot 376}{\sum N_n} = \frac{\sum N_n \cdot (n \cdot 47)}{\sum N_n} \tag{6}$$

$N_n$ is the number of RF cluster types present in the simulation box, such that $N_1, N_2, \cdots N_8$, are the number of monomers, dimers, …, octamers, respectively. Hence, for our system, $0 \leq N_n \leq 8, N_n \in \mathbb{N}$ and $\sum N_n \leq 8$. The latter (divisor in equation (6) is denoted as the number of clusters present at one time ($N_{clust}$). Since one RF molecule consists of 47 atoms, the maximal aggregate size at one time is obviously 376 atoms, which corresponds to $N_{clust}$ of 1 and implies a single octameric cluster. The minimum aggregate size on the other hand equals 47 implying all RF molecules are dispersed, i.e. all in monomeric form, and the maximum number of clusters is reached ($N_{clust} = 8$).

Compared to the previous study in pure water in [25], the calculated average of number of cluster $< N_{clust} >$ showed generally smaller aggregate size (or vice versa more clusters) when the additives are included, which agrees with the experimental observation, see dashed lines Fig. 5 C. Additionally, the computation demonstrated that the interaction strength between the additive and RF depends significantly on the electronic structure of the additives. Cluster size analysis showed that electron donating groups, such as a methoxy group and a hydroxy group attached to the aromatic ring (see Fig. 5 C: Ferulate = black line, Na-4-OH-Cinn = red line and Na-3-OMe-Cinn = green line), enhanced the interaction between RF and the additive yielding significantly more dimeric and monomeric RF clusters in the system. This indicates that electrostatic interaction may also play a significant role in the solubilization process.

A saturated hydrocarbon group between the carboxylate group and the aromatic ring seems to be significantly detrimental to the solubilizing strength of the additive, again in accordance with the experiment, see Fig. 5 C: Na-4-OH-Prop = yellow line and Na-4-OH-Butyrate = brown line. We explain this by two effects: First, such a group interferes with charge delocalization. This would imply that delocalization of the negative charge of the carboxylate groups is decisive for the interaction. While this might be true for the electrostatics, dehydrogenation of the hydrocarbon chain and delocalization of charge induce planarization of the molecular system. π-π interactions are known to scale linearly with the surface area of interaction, and hence larger surface available in the additive should increase the magnitude of the interaction. The saturation of the hydrocarbon chain in Na-4-OH-Prop and Na-4-OH-Butyrate reduced the effective surface of the additive due to folding of the corresponding moiety. Additionally, the presence of saturated groups counteracts aggregation between the aryl derivative and RF because the entropic penalty increases due to reduced flexibility. Hence, torsional restraint applied to Na-4-OH-Prop on the saturated moiety leads to remarkably smaller RF clusters present in the system (6.45) compared to the unmodified additive (2.43). Hence, a cluster analysis of the MD simulation of RF in presence of various polyphenolate(−like) molecules showed smaller aggregate sizes of RF in presence of electron-richer planar polyphenolate(−like) molecules. This correlates with the fact that lower polyphenolate/RF ratios were required to solubilize RF with electron-richer polyphenolate(−like) molecules in real life experiments from Section 3.1.

The modulation of electrostatic attractive force may lead to a different hydrogen bond strength between RF and the additives. However, current results did not indicate that the number of hydrogen bonds (HBnum) during the 700 ns MD simulation correlates with the RF aggregate size, see Table A 84 in Supplementary Material. While a slight correlation between aggregate size and HBnum in the row of delocalized additives (Ferulate > Na-4-OH-Cinn ~ Na-3-OMe-Cinn > NaCinn) can be observed, the trend does not hold for Na-4-OH-Prop and Na-4-OH-Butyrate. While the hydrogenation of the vinyl moiety of Na-4-OH-Cinn into Na-4-OH-Prop leads clearly to weaker solubilizing strength as an additive, hydrogen bond numbers between RF/Na-4-OH-Cinn or RF/Na-4-OH-Prop are practically comparable. This leads to the conclusion that hydrogen bonding is not decisive in the solubilizing process of RF.

To estimate the effect of polyphenolates in the solubilization of RF molecules, the free energy profile of the dissociation process of two RF molecules in the presence of 20 sodium ferulate molecules in water was calculated. Fig. 6 A clearly shows a significantly lower dissociation energy when ferulate molecules are included in the umbrella sampling simulation compared to the process in pure water (approximately 12.5 $kJ \cdot mol^{-1}$ lower), which is in line with the smaller aggregate size number found from the cluster analysis, see Fig. 5 C.

The low molar sodium ferulate/RF ratios observed during hydrotropic solubilization of RF with ferulate from Section 3.1, correlates with the outcome of the umbrella sampling of RF with 20 sodium ferulate molecules that showed a significant decrease of RF's dissociation energy due to sodium ferulate. This confirms once more, that RF's solubilization is limited by RF-RF π-stacking and hints to π-stacking interactions between RF and polyphenolates.

In addition to the lower separation energy, the profile showed several local minima (ζ = 0.6 nm and 0.75 nm) along the COM-

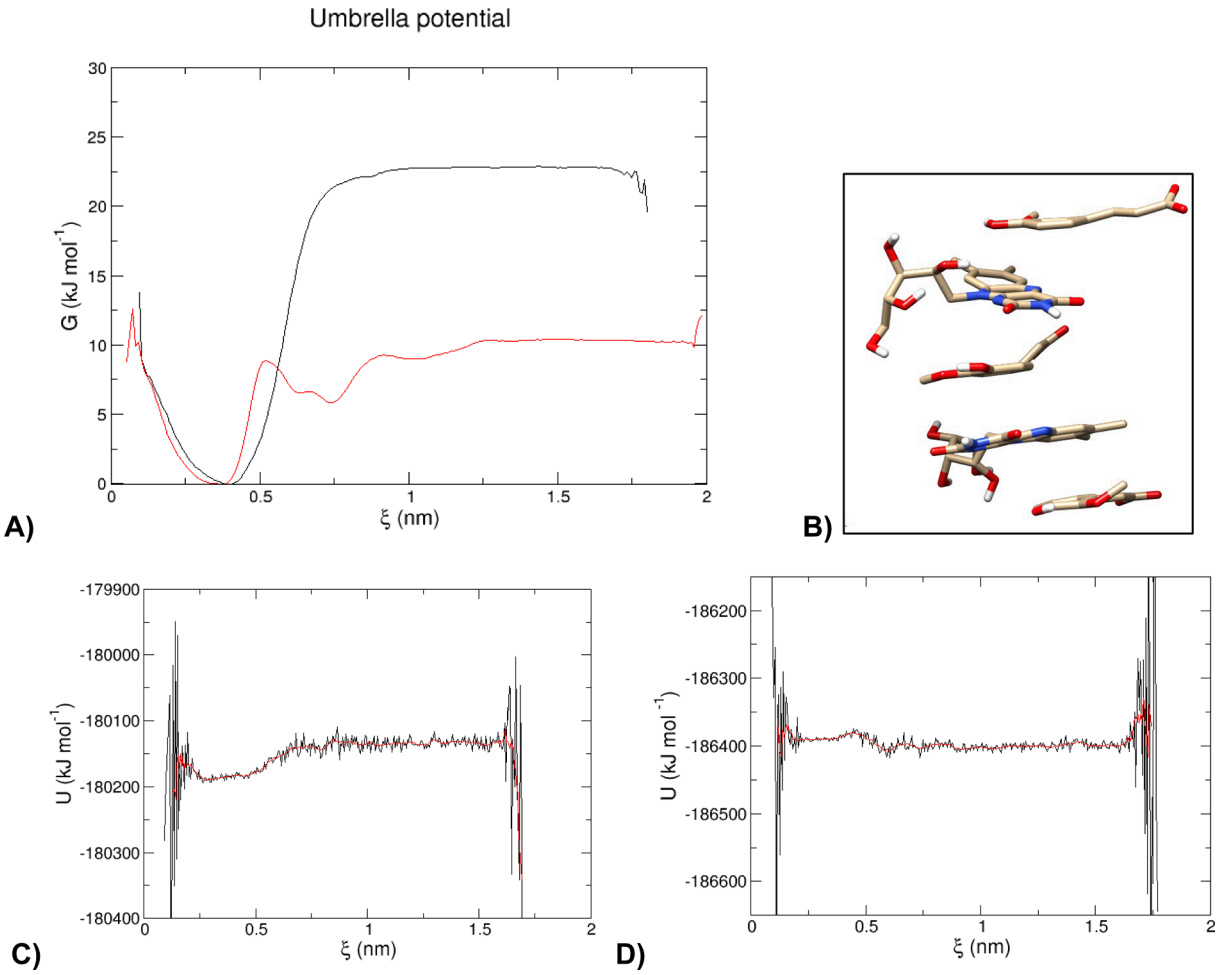


**Fig. 6.** (A) PMF extracted from umbrella sampling for the dissociation of two riboflavin molecules in pure water (black line; [25]) compared to the profile in water with 20 additional sodium ferulate molecules (red line). (B) Snapshot of trajectory from sampling at riboflavin separation COM distance 0.75 nm. (C) Internal energy profile along the pulling coordinates in pure water, and (D) in the presence of 20 sodium ferulate molecules. (For interpretation of the references to color in this figure legend, the reader is referred to the web version of this article.)

separation axis, which may suggest the formation of either different stacking arrangement between two RF molecules or an intermediate with a ferulate molecule inserted in between the two RF molecules, see Fig. 6 B. However, whether the intermediates formed in the pathway contribute positively (kinetically or thermodynamically) to the separation process is a subject of further investigation. Finally, we performed thermodynamic analysis of the dissociation process by separating the thermodynamic potentials into enthalpy $H$ or internal energy $U$ and entropy $S$. Since $U$ and $H$ are just related by the term $pV$ and the simulation was carried out on an equilibrated system at constant pressure, $U$ is approximately $H$ in this case. Generally, to estimate the change in state functions, generating the Van't Hoff plot by performing umbrella sampling of the separation process at different temperatures is straightforward. However, such calculations are very expensive and dependent on the response nature of the reaction towards temperature change at constant pressure. Instead of repeating the umbrella sampling at various temperatures, binning of internal energy as a function of pulling coordinates (COM) was performed. Due to poor signal to noise ratio, exact quantification of enthalpy/internal energy is impossible. Nevertheless, a clear trend and rough estimates can be obtained from the binning procedure.

Fig. 6 C and D showed that the dissociation process in the presence of sodium ferulate is mildly exothermic (DH $\sim -10$ kJ·mol$^{-1}$), while the same process in pure water is largely endothermic (DH $\sim +50$ kJ·mol$^{-1}$). Since DG (+22.8 kJ·mol$^{-1}$) in the latter case is smaller than DH, the reaction at room temperature is entropically driven (DS $> 0$). For the former case, the sign of DS is indeed inverted, because DG $> 0$ and DH $< 0$. Therefore, the dissociation process is rather enthalpically driven, in contrast to the case in pure water. Tentatively, this may suggest that the ferulate-riboflavin complex formation is enthalpically favorable, facilitating the dissolution of RF aggregates, however, it comes at the cost of the overall system entropy.

## 4. Conclusion

In accordance to [25], separation of the electrostatic and dispersive interaction term of RF with other RF molecules suggests dispersion as reason for RF's limited water solubility. Sodium/choline polyphenolates turned out as efficient hydrotropes for RF – being more efficient than the typical salting-in agent NaSCN, the typical hydrotrope sodium xylene sulfonate, the surfactant sodium dodecyl sulfate, and even more efficient than the well-known RF solubilizer nicotinamide [30]. RF's water solubility increased exponentially with the polyphenolate concentration. Due to higher water solubility, choline polyphenolates solubilized more RF than sodium polyphenolates, but were slightly less efficient than the sodium salts. Sodium polyphenolates enabled minimum molar polyphenolate/RF ratios of 6.3–4.2. Although hydration and amphiphilicity were not insignificant for the solubilization of RF, the size and type of the conjugated π-electron system were decisive for the polyphenolates' solubilizing performance. The water solubility of polyphenolates did not

correlate with their RF solubilizing efficiency.

(i) Comparison of the solubilization efficiencies of distinct aromatic/semi- and non-aromatic sodium carboxylates, (ii) NMR measurements, and (iii) molecular dynamics confirmed π-stacking of RF and sodium polyphenolates to be responsible for the hydrotropic effect of polyphenolates. Hence, mainly RF's isoalloxazine ring participates in the interaction with polyphenolates. This is in line with the comparable hydrotropic effect of polyphenolates on the lumichrome and riboflavin 5′-monophosphate reported in [74]. Umbrella sampling and cluster analysis of RF in the presence of sodium ferulate indicated the formation of different aggregates of RF with sodium ferulate and a reduction of the average RF cluster size. Deeper analysis of the Gibbs energy proposed RF's dissociation in pure water to be entropically driven, while it is enthalpically favored in an aqueous polyphenolate solution at the cost of the overall entropy of the system.

MD simulations and NMR measurements indicated an influence of polyphenolates on the ribityl chain conformation. Stacking might induce a change of the average ribityl chain conformation. An altered ribityl chain might reinforce the hydrotropic effect of polyphenolates.

In a recent article, we showed the hydrotropic effect of polyphenolates on di(propylene glycol) n-propyl ether (DPnP). Contrary to the hydrotropic effect of aromatic carboxlyates on RF, DPnP's solubilization was based on the aromatic sodium carboxylate's amphiphilicity. Thus, aromatic sodium carboxylates exert at least two distinct solubilizing modes in aqueous solution. Both solubilization processes underly specific molecular interactions and are not dominated by classical aggregation of the hydrotrope around the solute such as in surfactant based systems [2,13,51]. This finding correlates with Bauduin's observation that the hydrophobic surface is not the only important property of hydrotropes [81]. As polyphenolates exert at least two distinct modes of hydrotropy and because their conjugated acids are known to complex second group metal cations, subsequent studies should deal with the effect of metal cations on the polyphenolates' hydrotropic abilities [82].

The reversible complex formation of RF and polyphenolates might enable the formulation of a nutraceutical, in which the polyphenolates' antioxidant properties might prevent the deactivation of RF's vitamin function via oxidation.

As the redox potential of RF can be influenced by π-stacking, polyphenolates might be even able to influence biological processes [83]. Hence, being part of the human's daily nutrition, and being widely distributed in the plant kingdom, polyphenolates and their conjugated acids might play a secondary role as multifunctional biological solubilizers.

## CRediT authorship contribution statement

**Nadja Ulmann:** Writing – review & editing, Writing – original draft, Visualization, Validation, Project administration, Methodology, Investigation, Formal analysis, Data curation, Conceptualization. **Johnny Hioe:** Writing – review & editing, Writing – original draft, Visualization, Validation, Software, Methodology, Investigation, Formal analysis, Data curation, Conceptualization. **Didier Touraud:** Writing – review & editing, Writing – original draft, Supervision, Project administration, Methodology, Conceptualization. **Eva Müller:** Writing – original draft, Validation, Conceptualization. **Dominik Horinek:** Writing – review & editing, Writing – original draft, Supervision, Software, Methodology, Conceptualization. **Werner Kunz:** Writing – review & editing, Writing – original draft, Supervision, Resources, Project administration, Funding acquisition, Conceptualization.

## Declaration of competing interest

The authors declare the following financial interests/personal relationships which may be considered as potential competing interests: Werner Kunz, Nadja Ulmann reports financial support was provided by BASF SE. If there are other authors, they declare that they have no known competing financial interests or personal relationships that could have appeared to influence the work reported in this paper.

## Acknowledgements

We thank Julian Schiller, Martin Rosenhammer, and Hugo Cuvilliers for the conduction of a part of the experimental section. This work was partially funded by BASF SE. We also thank the NMR department of the University of Regensburg for enabling the NMR measurements.

## Appendix A. Supplementary data

[84,85,86,87,88,89,90,91,92,93,94,95,96]. Supplementary data to this article can be found online at https://doi.org/10.1016/j.molliq.2025.127465.

## Data availability

No data was used for the research described in the article.

## References

[1] Water Science School, The Water in You: Water and the Human Body, (2019). https://www.usgs.gov/special-topics/water-science-school/science/water-you-water-and-human-body#:~:text=In adult men%2C about 60,their bodies made of water (Accessed August 5, 2024).
[2] W. Kunz, K. Holmberg, T. Zemb, Hydrotropes, Curr. Opin. Colloid Interface Sci. 22 (2016) 99–107, https://doi.org/10.1016/j.cocis.2016.03.005.
[3] V. Larcinese-Hafner, V. Tchakalova, Co-surfactant, co-solvent, and hydrotropic properties of some common cooling agents, Flavour Fragr. J. 33 (2018) 303–312, https://doi.org/10.1002/ffj.3449.
[4] T. Ivanković, J. Hrenović, Surfactants in the environment, Arch. Ind. Hyg. Toxicol. 61 (2010) 95–110, https://doi.org/10.2478/10004-1254-61-2010-1943.
[5] T.K. Hodgdon, E.W. Kaler, Hydrotropic solutions, Curr. Opin. Colloid Interface Sci. 12 (2007) 121–128, https://doi.org/10.1016/j.cocis.2007.06.004.
[6] C. Neuberg, Hydrotropic phenomena, Biochem. z. 76 (1916) 107–108.
[7] N. Kapadiya, S. Indrajeet, M. Kushboo, K. Gauri, D. Sen, Hydrotropy: a promising tool for solubility enhancement: a review, Int. J. Drug Dev. Res. 3 (2011) 26–33.
[8] S. Das, S. Paul, Hydrotropic solubilization of sparingly soluble riboflavin drug molecule in aqueous nicotinamide solution, J. Phys. Chem. b. 121 (2017) 8774–8785, https://doi.org/10.1021/acs.jpcb.7b05774.
[9] D. Casey, K. Charalambous, A. Gee, R.V. Law, O. Ces, Amphiphilic drug interactions with model cellular membranes are influenced by lipid chain-melting temperature, J. R. Soc. Interface. 11 (2014), https://doi.org/10.1098/rsif.2013.1062.
[10] M.L. Klossek, D. Touraud, W. Kunz, Eco-solvents – cluster-formation, surfactantless microemulsions and facilitated hydrotropy, Phys. Chem. Chem. Phys. 15 (2013) 10971, https://doi.org/10.1039/c3cp50636c.
[11] S. Shimizu, N. Matubayasi, Hydrotropy: Monomer-micelle equilibrium and minimum hydrotrope concentration, J. Phys. Chem. b. 118 (2014) 10515–10524, https://doi.org/10.1021/jp505869m.
[12] J. Mehringer, E. Hofmann, D. Touraud, S. Koltzenburg, M. Kellermeier, W. Kunz, Salting-in and salting-out effects of short amphiphilic molecules: a balance between specific ion effects and hydrophobicity, Phys. Chem. Chem. Phys. 23 (2021) 1381–1391, https://doi.org/10.1039/D0CP05491G.
[13] M. Hopkins Hatzopoulos, J. Eastoe, P.J. Dowding, S.E. Rogers, R. Heenan, R. Dyer, Are hydrotropes distinct from surfactants? Langmuir 27 (2011) 12346–12353, https://doi.org/10.1021/la2025846.
[14] D.O. Abranches, J. Benfica, B.P. Soares, A. Leal-Duaso, T.E. Sintra, E. Pires, S. P. Pinho, S. Shimizu, J.A.P. Coutinho, Unveiling the mechanism of hydrotropy: evidence for water-mediated aggregation of hydrotropes around the solute, Chem. Commun. 56 (2020) 7143–7146, https://doi.org/10.1039/D0CC03217D.
[15] M.D. Dubbs, R.B. Gupta, Solubility of vitamin E (α-tocopherol) and vitamin K 3 (Menadione) in ethanol−water mixture, J. Chem. Eng. Data. 43 (1998) 590–591, https://doi.org/10.1021/je980017l.
[16] M. Sadauskas, R. Statkevičiūtė, J. Vaitekūnas, V. Petkevičius, V. Časaitė, R. Gasparavičiūtė, R. Meškys, Enzymatic synthesis of novel water-soluble indigoid compounds, Dye. Pigment. 173 (2020) 107882, https://doi.org/10.1016/j.dyepig.2019.107882.
[17] A. Etale, A.J. Onyianta, S.R. Turner, S.J. Eichhorn, Cellulose: a review of water interactions, applications in composites, and water treatment, Chem. Rev. 123 (2023) 2016–2048, https://doi.org/10.1021/acs.chemrev.2c00477.
[18] V. Dhapte, P. Mehta, Advances in hydrotropic solutions: an updated review, St. Petersbg. Polytech. Univ. J. Phys. Math. 1 (2015) 424–435, https://doi.org/10.1016/j.spjpm.2015.12.006.
[19] N. Suwannasom, I. Kao, A. Pruß, R. Georgieva, H. Bäumler, Riboflavin: the health benefits of a forgotten natural vitamin, Int. J. Mol. Sci. 21 (2020) 950, https://doi.org/10.3390/ijms21030950.

[20] C. Boehnke, U. Reuter, U. Flach, S. Schuh-Hofer, K.M. Einhaupl, G. Arnold, High-dose riboflavin treatment is efficacious in migraine prophylaxis: an open study in a tertiary care centre, Eur. J. Neurol. 11 (2004) 475–477, https://doi.org/10.1111/j.1468-1331.2004.00813.x.

[21] E.T. Marashly, S.A. Bohlega, Riboflavin has neuroprotective potential: focus on parkinson's disease and migraine, Front. Neurol. 8 (2017), https://doi.org/10.3389/fneur.2017.00333.

[22] L.A. Averianova, L.A. Balabanova, O.M. Son, A.B. Podvolotskaya, L.A. Tekutyeva, Production of vitamin B2 (Riboflavin) by microorganisms: an overview, Front. Bioeng. Biotechnol. 8 (2020), https://doi.org/10.3389/fbioe.2020.570828.

[23] D.B. McCormick, Two interconnected B vitamins: riboflavin and pyridoxine, Physiol. Rev. 69 (1989) 1170–1198, https://doi.org/10.1152/physrev.1989.69.4.1170.

[24] S. Balasubramaniam, J. Yaplito-Lee, Riboflavin metabolism: role in mitochondrial function, J. Transl. Genet. Genom. (2020) 286, https://doi.org/10.20517/jtgg.2020.34.

[25] N. Ulmann, W. Kunz, J. Hioe, D. Touraud, D. Horinek, Self-association as solubility limiting factor of riboflavin in aqueous medium, Phys. Chem. Chem. Phys. (2024), https://doi.org/10.1039/D4CP02074J.

[26] Future Market Insights, In Global Riboflavin Pigment Market, Developing Countries Will Offer the Best Growth Opportunities – Future Market Insights, Inc., GlobeNewswire. (2022). https://ca.sports.yahoo.com/news/global-riboflavin-pigment-market-developing-133000210.html?guccounter=1&guce_referrer=aHR0cHM6Ly93d3cuZ29vZ2xlLmNvbS8&guce_referrer_sig=AQAAAFxTm8j06RUwdIBbf8IOpW2okdXMYXhV-f56iOrvBkaFHLGqQlKknLN778BegWGgbkjqGPsuXgpAoyGHUd (Accessed October 8, 2022).

[27] World Health Organization, Codex Alimentarius, in: Gen. Stand. Food Addit., 2021, pp. 216–219. https://www.fao.org/fao-who-codexalimentarius/sh-proxy/en/?lnk=1&url=https%253A%252F%252Fworkspace.fao.org%252Fsites%252Fcodex%252FStandards%252FCXS%2B192-1995%252FCXS_192e.pdf.

[28] K.-P. Stahmann, J.L. Revuelta, H. Seulberger, Three biotechnical processes using Ashbya gossypii, Candida famata, or Bacillus subtilis compete with chemical riboflavin production, Appl. Microbiol. Biotechnol. 53 (2000) 509–516, https://doi.org/10.1007/s002530051649.

[29] W.H. Sebrell, R.S. Harris (Eds.), RIBOFLAVIN, in: Vitam., 2nd ed., Elsevier, 1972, pp. 1–96. doi: 10.1016/B978-0-12-633765-5.50008-3.

[30] R.E. Coffman, D.O. Kildsig, Effect of Nicotinamide and Urea on the Solubility of Riboflavin in Various Solvents, J. Pharm. Sci. 85 (1996) 951–954, https://doi.org/10.1021/js960012b.

[31] H.A. Staab, J. Kanellakopulos, P. Kirsch, C. Krieger, π…π interactions of flavins, 5. Syntheses, structures and physical properties of flavin systems with covalent bonding to π donors and π acceptors (quinones), Liebigs Ann. (1995) 1827–1836, https://doi.org/10.1002/jlac.1995199510256.

[32] S. Fujii, K. Kawasaki, A. Sato, T. Fujiwara, K.-I. Tomita, Crystal and molecular structure of a 1:1 molecular complex of adenine and riboflavin, Arch. Biochem. Biophys. 181 (1977) 363–370, https://doi.org/10.1016/0003-9861(77)90241-7.

[33] I. Ahmad, Effect of nicotinamide on the photolysis of riboflavin in aqueous solution, Sci. Pharm. 84 (2016) 289–303, https://doi.org/10.3797/scipharm.1507-04.

[34] M.A. Sheraz, S.H. Kazi, S. Ahmed, Z. Anwar, I. Ahmad, Photo, thermal and chemical degradation of riboflavin, Beilstein J. Org. Chem. 10 (2014) 1999–2012, https://doi.org/10.3762/bjoc.10.208.

[35] W.J. Peterson, F.M. Haig, A.O. Shaw, Destruction of riboflavin in milk by sunlight, J. Am. Chem. Soc. 66 (1944) 662–663, https://doi.org/10.1021/ja01232a515.

[36] D.R. Cardoso, K. Olsen, J.K.S. Møller, L.H. Skibsted, Phenol and terpene quenching of singlet- and triplet-excited states of riboflavin in relation to light-struck flavor formation in beer, J. Agric. Food Chem. 54 (2006) 5630–5636, https://doi.org/10.1021/jf060750d.

[37] M.R. Goldsmith, P.J. Rogers, N.M. Cabral, K.P. Ghiggino, F.A. Roddick, Riboflavin Triplet Quenchers Inhibit Lightstruck Flavor Formation in Beer, J. Am. Soc. Brew. Chem. 63 (2005) 177–184, https://doi.org/10.1094/ASBCJ-63-0177.

[38] M.K. Mishra, A. Mukherjee, U. Ramamurty, G.R. Desiraju, Crystal chemistry and photomechanical behavior of 3,4-dimethoxycinnamic acid: correlation between maximum yield in the solid-state topochemical reaction and cooperative molecular motion, IUCrJ. 2 (2015) 653–660, https://doi.org/10.1107/S2052252515017297.

[39] J. Nishijo, I. Yonetani, Interaction of theobromine with sodium benzoate, J. Pharm. Sci. 71 (1982) 354–356, https://doi.org/10.1002/jps.2600710324.

[40] M. Vraneš, T.T. Borović, P. Drid, T. Trivić, R. Tomaš, N. Janković, Influence of sodium salicylate on self-aggregation and caffeine solubility in water—a new hypothesis from experimental and computational data, Pharmaceutics 14 (2022) 2304, https://doi.org/10.3390/pharmaceutics14112304.

[41] S. Datta, C. Mukhopadhyay, S.K. Bose, Molecular complex formation between riboflavin and salicylate in an aqueous medium, Bull. Chem. Soc. Jpn. 76 (2003) 1729–1734, https://doi.org/10.1246/bcsj.76.1729.

[42] J. Chen, J. Yang, L. Ma, J. Li, N. Shahzad, C.K. Kim, Structure-antioxidant activity relationship of methoxy, phenolic hydroxyl, and carboxylic acid groups of phenolic acids, Sci. Rep. 10 (2020) 2611, https://doi.org/10.1038/s41598-020-59451-z.

[43] EFSA J. 10 (2012), https://doi.org/10.2903/j.efsa:2012.2994.

[44] J.A. Hoskins, The occurrence, metabolism and toxicity of cinnamic acid and related compounds, J. Appl. Toxicol. 4 (1984) 283–292, https://doi.org/10.1002/jat.2550040602.

[45] M.N. Clifford, Chlorogenic acids and other cinnamates - nature, occurrence and dietary burden, J. Sci. Food Agric. 79 (1999) 362–372, https://doi.org/10.1002/(SICI)1097-0010(19990301)79:3<362::AID-JSFA256>3.0.CO;2-D.

[46] J.C. Bird, A. Kuna, Aqueous Solution of Riboflavin 534 (1946) 826. https://patents.google.com/patent/US2407624A/en.

[47] M. Karmazyn, X.T. Gan, R.A. Humphreys, H. Yoshida, K. Kusumoto, The myocardial Na + -H + exchange, Circ. Res. 85 (1999) 777–786, https://doi.org/10.1161/01.RES.85.9.777.

[48] L. Shi, M. Quick, Y. Zhao, H. Weinstein, J.A. Javitch, The mechanism of a neurotransmitter:sodium symporter—inward release of Na+ and substrate is triggered by substrate in a second binding site, Mol. Cell. 30 (2008) 667–677, https://doi.org/10.1016/j.molcel.2008.05.008.

[49] S.H. Zeisel, K.-A. da Costa, Choline: an essential nutrient for public health, Nutr. Rev. 67 (2009) 615–623, https://doi.org/10.1111/j.1753-4887.2009.00246.x.

[50] T.E. Sintra, A. Luís, S.N. Rocha, A.I.M.C. Lobo Ferreira, F. Gonçalves, L.M.N.B. F. Santos, B.M. Neves, M.G. Freire, S.P.M. Ventura, J.A.P. Coutinho, Enhancing the antioxidant characteristics of phenolic acids by their conversion into cholinium salts, ACS Sustain Chem. Eng. 3 (2015) 2558–2565, https://doi.org/10.1021/acssuschemeng.5b00751.

[51] N. Ulmann, K. Häckl, D. Touraud, W. Kunz, Investigation of the salting-in/-out, hydrotropic and surface-active behavior of plant-based hormone and phenolic acid salts, J. Colloid Interface Sci. 641 (2023) 631–642, https://doi.org/10.1016/j.jcis.2023.03.077.

[52] M.L. Klossek, D. Touraud, T. Zemb, W. Kunz, Structure and solubility in surfactant-free microemulsions, ChemPhysChem 13 (2012) 4116–4119, https://doi.org/10.1002/cphc.201200667.

[53] S. Páll, M.J. Abraham, C. Kutzner, B. Hess, E. Lindahl, Tackling exascale software challenges in molecular dynamics simulations with GROMACS, 2015, pp. 3–27. doi: 10.1007/978-3-319-15976-8_1.

[54] M.J. Abraham, T. Murtola, R. Schulz, S. Páll, J.C. Smith, B. Hess, E. Lindahl, GROMACS: high performance molecular simulations through multi-level parallelism from laptops to supercomputers, SoftwareX. 1–2 (2015) 19–25, https://doi.org/10.1016/j.softx.2015.06.001.

[55] S. Pronk, S. Páll, R. Schulz, P. Larsson, P. Bjelkmar, R. Apostolov, M.R. Shirts, J. C. Smith, P.M. Kasson, D. Spoel, B. Hess, E. Lindahl, GROMACS 4.5: a high-throughput and highly parallel open source molecular simulation toolkit, Bioinformatics 29 (2013) 845–854, https://doi.org/10.1093/bioinformatics/btt055.

[56] B. Hess, C. Kutzner, D. van der Spoel, E. Lindahl, GROMACS 4: algorithms for highly efficient, load-balanced, and scalable molecular simulation, J. Chem. Theory Comput. 4 (2008) 435–447, https://doi.org/10.1021/ct700301q.

[57] D. Van Der Spoel, E. Lindahl, B. Hess, G. Groenhof, A.E. Mark, H.J.C. Berendsen, GROMACS: fast, flexible, and free, J. Comput. Chem. 26 (2005) 1701–1718, https://doi.org/10.1002/jcc.20291.

[58] E. Lindahl, B. Hess, D. Spoel, GROMACS 3.0: a package for molecular simulation and trajectory analysis, J. Mol. Model. 7 (2001) 306–317, https://doi.org/10.1007/s008940100045.

[59] H.J.C. Berendsen, D. van der Spoel, R. van Drunen, GROMACS: a message-passing parallel molecular dynamics implementation, Comput. Phys. Commun. 91 (1995) 43–56, https://doi.org/10.1016/0010-4655(95)00042-E.

[60] P. Bauer, B. Hess, E. Lindahl, GROMACS 2022 Source code, (2022). doi: doi: 10.5281/zenodo.6103835.

[61] J. Wang, W. Wang, P.A. Kollman, D.A. Case, Automatic atom type and bond type perception in molecular mechanical calculations, J. Mol. Graph. Model. 25 (2006) 247–260, https://doi.org/10.1016/j.jmgm.2005.12.005.

[62] J. Wang, R.M. Wolf, J.W. Caldwell, P.A. Kollman, D.A. Case, Development and testing of a general amber force field, J. Comput. Chem. 25 (2004) 1157–1174, https://doi.org/10.1002/jcc.20035.

[63] A.W. Sousa da Silva, W.F. Vranken, ACPYPE - AnteChamber PYthon Parser interfacE, BMC Res. Notes. 5 (2012) 367, https://doi.org/10.1186/1756-0500-5-367.

[64] R. Woods, R. Chappelle, Restrained electrostatic potential atomic partial charges for condensed-phase simulations of carbohydrates, J. Mol. Struct. Theochem. 527 (2000) 149–156, https://doi.org/10.1016/S0166-1280(00)00487-5.

[65] Y. Zhao, D.G. Truhlar, The M06 suite of density functionals for main group thermochemistry, thermochemical kinetics, noncovalent interactions, excited states, and transition elements: two new functionals and systematic testing of four M06-class functionals and 12 other function, Theor. Chem. Acc. 120 (2008) 215–241, https://doi.org/10.1007/s00214-007-0310-x.

[66] F. Weigend, F. Furche, R. Ahlrichs, Gaussian basis sets of quadruple zeta valence quality for atoms H–Kr, J. Chem. Phys. 119 (2003) 12753–12762, https://doi.org/10.1063/1.1627293.

[67] F. Weigend, R. Ahlrichs, Balanced basis sets of split valence, triple zeta valence and quadruple zeta valence quality for H to Rn: Design and assessment of accuracy, Phys. Chem. Chem. Phys. 7 (2005) 3297, https://doi.org/10.1039/b508541a.

[68] F. Neese, The ORCA program system, Wires Comput. Mol. Sci. 2 (2012) 73–78, https://doi.org/10.1002/wcms.81.

[69] F. Neese, F. Wennmohs, A. Hansen, U. Becker, Efficient, approximate and parallel Hartree–Fock and hybrid DFT calculations. A 'chain-of-spheres' algorithm for the Hartree–Fock exchange, Chem. Phys. 356 (2009) 98, https://doi.org/10.1016/j.chemphys.2008.10.036.

[70] G. Bussi, D. Donadio, M. Parrinello, Canonical sampling through velocity rescaling, J. Chem. Phys. 126 (2007) 014101, https://doi.org/10.1063/1.2408420.

[71] M. Bernetti, G. Bussi, Pressure control using stochastic cell rescaling, J. Chem. Phys. 153 (2020) 114107, https://doi.org/10.1063/5.0020514.

[72] S. Kumar, J.M. Rosenberg, D. Bouzida, R.H. Swendsen, P.A. Kollman, The weighted histogram analysis method for free-energy calculations on biomolecules. I. The method, J. Comput. Chem. 13 (1992) 1011–1021, https://doi.org/10.1002/jcc.540130812.

[73] W. Wang, J.J. Han, L.Q. Wang, L.S. Li, W.J. Shaw, A.D.Q. Li, Dynamic π-π stacked molecular assemblies emit from green to red colors, Nano Lett. 3 (2003) 455–458, https://doi.org/10.1021/nl025976j.
[74] N. Ulmann, Solubilization and Stabilization of Natural Molecules in Green and Edible Formulations, University of Regensburg, 2023.
[75] S. Shan, D. Herschlag, The change in hydrogen bond strength accompanying charge rearrangement: Implications for enzymatic catalysis, Proc. Natl. Acad. Sci. 93 (1996) 14474–14479, https://doi.org/10.1073/pnas.93.25.14474.
[76] N. Agarwal, M.S. Nair, A. Mazumder, K.M. Poluri, Characterization of nanomaterials using nuclear magnetic resonance spectroscopy, Elsevier Ltd., (2018), https://doi.org/10.1016/B978-0-08-101973-3.00003-1.
[77] S.I. Yusa, Polymer characterization, Polym. Sci. Nanotechnol. Fundam. Appl. (2020) 105–124, https://doi.org/10.1016/B978-0-12-816806-6.00006-6.
[78] L. Chen, H. Wang, J. Liu, R. Xing, X. Yu, Y. Han, Tuning the π-π stacking distance and J-aggregation of DPP-based conjugated polymer via introducing insulating polymer, J. Polym. Sci. Part B Polym. Phys. 54 (2016) 838–847, https://doi.org/10.1002/polb.23984.
[79] Y. Zhao, E.S. Sarnello, L.A. Robertson, J. Zhang, Z. Yu, Z. Shi, S.R.Z. Y. Bheemireddy, T. Li, R.S. Assary, L. Cheng, Z. Zhang, L. Zhang, I.A. Shkrob, Competitive pi-stacking and H-bond piling increase solubility of heterocyclic redoxmers, J. Phys. Chem. b. 124 (2020) 10409–10418, https://doi.org/10.1021/acs.jpcb.0c07647.
[80] J.-H. Deng, J. Luo, Y.-L. Mao, S. Lai, Y.-N. Gong, D.-C. Zhong, T.-B. Lu, π-π stacking interactions: non-negligible forces for stabilizing porous supramolecular frameworks, Sci. Adv. 6 (2020), https://doi.org/10.1126/sciadv.aax9976.
[81] P. Bauduin, A. Renoncourt, A. Kopf, D. Touraud, W. Kunz, Unified concept of solubilization in water by hydrotropes and cosolvents, Langmuir 21 (2005) 6769–6775, https://doi.org/10.1021/la050554l.
[82] Z. Zhao, M. Vavrusova, L.H. Skibsted, Antioxidant activity and calcium binding of isomeric hydroxybenzoates, J. Food Drug Anal. 26 (2018) 591–598, https://doi.org/10.1016/j.jfda.2017.07.001.
[83] B. Henriques, V.R. Preedy, Riboflavin and β-oxidation flavoenzymes, in: B Vitam. Folate Chem. Anal. Funct. Eff.,, Royal Society of Chemistry, 2012, pp. 611–632, https://doi.org/10.1039/9781849734714.
[84] C.V. Subbarao, I.P.K. Chakravarthy, A.V.S.L. Sai Bharadwaj, K.M.M. Prasad, Functions of hydrotropes in solutions, Chem. Eng. Technol. 35 (2012) 225–237, https://doi.org/10.1002/ceat.201100484.
[85] Y. Kwon, Theoretical study on salicylic acid and its analogues: intramolecular hydrogen bonding, J. Mol. Struct. Theochem. 532 (2000) 227–237, https://doi.org/10.1016/S0166-1280(00)00555-8.
[86] D.R. Kammerer, Anthocyanins, in: Handb. Nat. Pigment. Food Beverages, Elsevier, 2016, pp. 61–80. doi: 10.1016/B978-0-08-100371-8.00003-8.
[87] A. Morata, C. López, W. Tesfaye, C. González, C. Escott, Anthocyanins as natural pigments in beverages, in: Value-Added Ingredients and Enrichments of Beverages, Elsevier, 2019, https://doi.org/10.1016/B978-0-12-816687-1.00012-6, pp. 383–428.
[88] P. Trouillas, J.C. Sancho-García, V. De Freitas, J. Gierschner, M. Otyepka, O. Dangles, Stabilizing and modulating color by copigmentation: insights from theory and experiment, Chem. Rev. 116 (2016) 4937–4982, https://doi.org/10.1021/acs.chemrev.5b00507.
[89] K. Undheim, T. Benneche, Pyrimidines and their Benzo Derivatives, in: Compr. Heterocycl. Chem. II, Elsevier, 1996, p. 97. doi: 10.1016/B978-008096518-5.00118-0.
[90] R. Winkler, T. Buchecker, F. Hastreiter, D. Touraud, W. Kunz, PPh4Cl in aqueous solution – the aggregation behavior of an antagonistic salt, Phys. Chem. Chem. Phys. 19 (2017) 25463–25470, https://doi.org/10.1039/C7CP02677C.
[91] S. Bienz, Vorlesungsskript zu Anwendung Spektroskopischer Methoden Teil, Kernmagnetische Resonanz (2002). https://www.chem.uzh.ch/dam/jcr:3bb1a31a-bd33-48af-80b0-ddfad7c5d4ee/_NMR_Skript_Bienz.pdf.
[92] W. Römisch, W. Eisenreich, G. Richter, A. Bacher, Rapid one-pot synthesis of riboflavin isotopomers, J. Org. Chem. 67 (2002) 8890–8894, https://doi.org/10.1021/jo026105x.
[93] A.M. Edwards, A. Saldaño, C. Bueno, E. Silva, S. Alegría, Spectroscopic properties of hydrophobic flavin esters.: a one and two-dimensional $^{1}$H-NMR and 13C-NMR study, Boletín La Soc. Chil. Química. 45 (2000), https://doi.org/10.4067/S0366-16442000000300013.
[94] T. Kim, S.Y. Park, M.-H. Lee, D.-H. Kim, I. Chung, Syntheses of polyrotaxane conjugated with 5-fluorouracil and vitamins with improved antitumor activities, J. Bioact. Compat. Polym. 34 (2019) 25–38, https://doi.org/10.1177/0883911518813617.
[95] R. Ellson, R. Stearns, M. Mutz, C. Brown, B. Browning, D. Harris, S. Qureshi, J. Shieh, D. Wold, In situ DMSO hydration measurements of HTS compound libraries, Comb. Chem. High Throughput Screen. 8 (2005) 489–498, https://doi.org/10.2174/1386207054867382.
[96] K.-I. Oh, K. Rajesh, J.F. Stanton, C.R. Baiz, Quantifying hydrogen-bond populations in dimethyl sulfoxide/water mixtures, Angew. Chem. Int. Ed. 56 (2017) 11375–11379, https://doi.org/10.1002/anie.201704162.